Materials Horizons

ROYAL SOCIETY OF CHEMISTRY

REVIEW

View Article Online
View Journal | View Issue

Cite this: *Mater. Horiz.*, 2025, **12**, 2789

From 3D to 4D printing of lignin towards green materials and sustainable manufacturing

Tingting Wu,[a] Sigit Sugiarto,[a] Ruochen Yang,[a] Thenapakiam Sathasivam,[a] Udyani Aloka Weerasinghe,[bc] Pei Lin Chee,[b] Odelia Yap,[d] Gustav Nyström*[ef] and Dan Kai*[abc]

Lignin is the second most abundant renewable and sustainable biomass resource. Developing advanced manufacturing to process lignin/lignocellulose into functional materials could reduce the consumption of petroleum-based materials. 3D printing provides a promising strategy to realize complex and customized geometries of lignin materials. The heterogeneity and complexity of lignin hinder its processing *via* additive manufacturing, but the recent advancement in lignin modification and polymerization provides new opportunities. Here, we summarize the recent state-of-the-art 3D printing of lignin materials, including the selection and formulation of lignin materials based on different printing techniques, the chemical modification of lignin for enhanced printability, and the related application fields. Additionally, we highlight the significant role of the 3D printing of lignocellulose biomass materials, such as wood powder and agricultural wastes. It was concluded that the most challenging part is to enhance the printability of lignin materials through modification and pretreatment of lignin while keeping the whole process green and sustainable. Beyond 3D printing, we further discuss the development of smart lignin materials and their potential for 4D printing. Ultimately, we discuss the current challenges and potential opportunities for the additive manufacturing of lignin materials. We believe this review can raise awareness among researchers about the potential of lignin materials as whole materials for constructing blocks and can promote the development of 3D/4D printing of lignin towards sustainability.

Received 22nd November 2024,
Accepted 22nd January 2025

DOI: 10.1039/d4mh01680g

rsc.li/materials-horizons

Wider impact

3D/4D printing of lignin materials has been extensively studied, with a particular focus on thermoplastic polymer/lignin composites for fused deposition modeling (FDM) and resin/lignin composites for stereolithography (SLA). The primary aim of incorporating lignin is to replace petroleum-derived materials while improving the performance of 3D-printed products, leveraging lignin's abundance and renewability. However, challenges such as interfacial defects between lignin and the matrix have limited its incorporation and, in some cases, adversely affected the performance of 3D-printed composites. Fortunately, lignin offers immense potential for chemical modification and copolymerization, which can address these interfacial issues while introducing ''smartness'' into 3D-printed lignin materials, enabling the transformation capabilities associated with 4D printing. In this review, we first discussed lignin modification, highlighting its pivotal role, before delving into the detailed 3D printing applications of lignin materials, aiming to inspire further exploration of lignin modification for 3D printing. Beyond commonly explored FDM and SLA, direct ink writing (DIW) presents a unique design approach, optimizing stable and homogeneous paste-like aqueous inks by tuning the interactions between lignin and water/media, often using bio-based fillers. Additionally, utilizing the full component of lignocellulosic biomass with minimal fillers in DIW represents a sustainable pathway for developing next-generation 3D-printed lignin-based materials.

[a] *Institute of Sustainability for Chemicals, Energy and Environment (ISCE^2), Agency for Science, Technology and Research (A*STAR), 1 Pesek Road, Jurong Island 627833, Singapore. E-mail: kaid@imre.a-star.edu.sg*
[b] *Institute of Materials Research and Engineering (IMRE), Agency for Science, Technology and Research (A*STAR), 2 Fusionopolis Way, Innovis #08-03, Singapore 138634, Singapore*
[c] *School of Chemistry, Chemical Engineering and Biotechnology, Nanyang Technological University, 21 Nanyang Link, Singapore 637371, Singapore*
[d] *School of Civil and Environmental Engineering, Nanyang Technological University, N1-01a-29, 50 Nanyang Avenue, Singapore 639798, Singapore*
[e] *Cellulose & Wood Materials Laboratory, Empa, Überlandstrasse 129, CH-8600, Dübendorf, Switzerland. E-mail: gustav.nystroem@empa.ch*
[f] *Department of Health Science and Technology, ETH Zürich, Schmelzbergstrasse 9, CH-8092, Zürich, Switzerland*

1. Introduction

The durability of petroleum-based polymer materials, attributed to their intrinsic chemical and physical stability, has enabled their widespread application in daily life. However, they also cause serious end-of-life environmental concerns. Therefore, numerous efforts have been made to search for bio-based, renewable, and compostable replacements to mitigate environmental problems.[1–3] Among them, lignocellulosic biomass is a promising candidate due to its abundance, renewability, and biodegradability.[4–7]

There are three major components of lignocellulosic biomass: cellulose, hemicellulose, and lignin. Among them, cellulose is the most widely investigated. Lignin is the second most abundant renewable and sustainable biomass resource after cellulose (around 15–30% of all lignocellulosic biomass materials) and is the principal biological source of aromatic polymers.[8–10] Around 50 million tons of lignin are produced annually globally, and its complex structures strongly depend on the origin of plant species and the isolation process. Because of its unique chemical structures and properties, lignin has attracted significant attention from researchers. However, lignin is still mostly regarded as the by-product or industrial waste of the cellulose extraction process used in the pulp industry. Currently, the by-product lignin remains underutilized and is mainly used for incineration and as a biofuel to

Tingting Wu

*Dr Tingting Wu is a Scientist at the A*STAR Institute of Sustainability for Chemicals, Energy and Environment (ISCE²), specializing in the deep eutectic solvent treatment of lignocellulose biomass and its 3D printing. She worked as a Postdoc at the Swiss Federal Laboratory for Materials Science and Technology (Empa) from February 2021 to June 2023, focusing on 3D-printed polyimide composite aerogels and hydrophobic cellulose foams. She earned her PhD from Donghua University in 2021, developing polyimide aerogels as thermal insulation and low-dielectric materials. She has worked at Empa as a visiting PhD on cellulose nanofibril-based aerogels and the colloidal interaction between cellulose nanofibrils and proteins.*

Sigit Sugiarto

*Sigit Sugiarto is a Senior Research Engineer at the Institute of Sustainability for Chemicals, Energy and Environment (ISCE²), A*STAR. He received his BSc in Chemistry from the National University of Singapore in 2017. Sigit specializes in the chemical functionalization of biomass-derived molecules, focusing on developing advanced functional materials, including lignin-based polymers.*

Gustav Nyström

Gustav Nyström received his PhD in engineering physics from Uppsala University, Sweden, in 2012. Following postdoctoral work at the KTH Royal Institute of Technology (Stockholm) and ETH Zurich, Switzerland, where he focused on fundamental studies of nanocellulose and amyloid fibril nanostructure characterization and liquid crystal self-assembly, he is now the Head of the Cellulose & Wood Materials laboratory at Empa (Dübendorf, Switzerland) and a Lecturer at ETH Zurich. His research is focused on three pillars – tailored biomass materials, digital cellulose technologies and materials from living systems – with the overall aim to develop a new generation of active, renewable, and more sustainable bio-based materials.

Dan Kai

*Dr Kai Dan is a Principal scientist at the Institute of Materials Research and Engineering & Institute of Sustainability for Chemicals, Energy and Environment, A*STAR. His research activities are focused on lignocellulosic materials and renewable materials, mainly on the chemical functionalization and advanced processing of biomass wastes (such as coconut husk, spent coffee grounds and lignin) towards high performance green composites and healthcare materials. He has demonstrated scientific excellence and technological achievements by publishing 100+ research papers in peer-reviewed journals, with a citation of ∼9900 and an h-index of 51.*

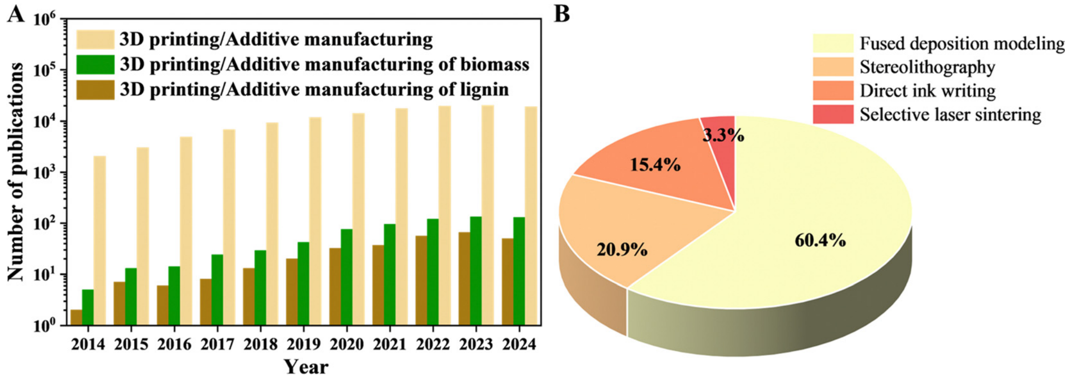

Fig. 1 (A) The number of publications on lignin additive manufacturing between 2014 and 2024. The data are obtained from the Web of Science on 20th November 2024. (B) Ratios of summarized publications in this review for lignin materials manufactured *via* different 3D printing techniques.

produce energy.[6] Therefore, the development of lignin valorization technology for high-value end applications is urgent and meaningful.

In recent years, widespread attention has been paid to upgrading the value of lignin towards development of advanced materials, such as films/membranes,[11] electrospun nanofibers,[12] and composites.[6] 3D printing, or additive manufacturing, is an efficient way to achieve customized and complex geometries for diverse application scenarios. Therefore, 3D printing is a promising technique that adds value to lignin in valorization.

There have been numerous attempts at lignin valorization *via* additive manufacturing to obtain lignin composites.[13,14] Lignin is adopted in variable polymer matrices for fused deposition modeling (FDM), such as poly(lactic acid) (PLA)[15,16] and polyhydroxybutyrate (PHB),[17] where lignin utilization aims to replace these petroleum-based polymers. Various properties of lignin, such as antioxidation and ultraviolet (UV)-blocking, have been explored to improve the functionality of 3D-printed lignin materials.[18] For example, the antioxidant capabilities of 3D-printed lignin/PLA composites were improved by adopting lignin.[15,19] Stereolithography (SLA) is another well-established technique for 3D printing lignin materials, based on the photopolymerization of light-sensitive resins.[20] The majority of these resins used are petroleum-derived. Thus, partial replacement of them with bio-sourced lignin is desirable. Direct ink writing (DIW) of lignin-based bio-inks is another technique often used to produce customized biomaterials. In those works, lignin is used in pure isolated or chemically modified form or as whole lignocellulose biomass. Among them, chemically modified lignin is the most efficient source for utilization in 3D printing, especially in FDM and SLA, as the chemical modification and copolymerization could improve the interfacial interaction between lignin and polymers and the dispersion of lignin, resulting in higher adoption volumes and more homogeneous dispersion. Therefore, the chemical modification and copolymerization of lignin will be discussed in this review.

3D printing or additive manufacturing of biomass and lignin has been increasingly studied in the last decade, and the publication numbers are shown in Fig. 1A. Fig. 1B demonstrates that most works on 3D-printed lignin materials involve the FDM technique, followed by the SLA technique. In the recently published reviews on 3D-printed lignocellulose biomass materials, the primary focus is on the general printing techniques and their properties, and the biomass materials adopted are mainly cellulose or lignin in isolated and purified forms and their corresponding composites.[5,21–23] Here, this review summarized the work on lignin/lignocellulose biomass materials for various 3D printing techniques, including fused deposition modeling (FDM), stereolithography (SLA), direct ink writing (DIW), and selective laser sintering (SLS), and their related applications, where lignin is used in an isolated state or as a part of lignocellulose biomass or is chemically modified to better bind with the matrix. For the FDM and SLA techniques, pristine lignin and chemically modified lignin or lignocellulose powders act as fillers in thermal plastic polymers and UV-curable resins, respectively, for the corresponding 3D printing. In the case of the DIW technique, lignin or lignocellulose biomass was mixed with other gel systems or additives to obtain mainly water-based paste-like inks for 3D printing. Additionally, 4D printing extends conventional 3D printing by introducing the dimension of time, enabling dynamic functionality in 3D-printed lignin-derived smart materials. These 4D-printed lignin materials can change their shapes, properties, or behaviors over time in response to external stimuli such as heat, light, humidity, or magnetic fields. By summarizing the relationships between lignin materials and printing techniques, their pros and cons, and the related application fields, we highlight the potential and underlying challenges of 3D/4D printing of lignin materials. Additionally, we evaluate the sustainability of lignin materials for 3D printing and potential considerations for future related research.

2. The modification and polymerization of lignin

Most lignin-based materials for 3D printing today rely on blending or composite approaches, which often result in heterogeneous structures and deteriorated properties. Due to the complexity and variability of the structure of lignin, its high variation in sizes, and poor compatibility with polymer matrices, it advocates the need for chemical modification.[24] Developing lignin-based copolymers through targeted modifications, including creating new chemically active sites, functionalizing hydroxyl groups, and copolymerizing lignin, can potentially create greater material homogeneity, enhancing compatibility and performance in advanced 3D printing applications. These alterations can be achieved through thermochemical, biochemical, or a combination of these approaches. This section will delve into these current chemical modification methods, their impact on lignin properties, and their potential to generate sustainable materials suitable for 3D/4D printing.

2.1. Creating chemically active sites

To obtain more value-added products, lignin can undergo further chemical modification to introduce additional chemically active sites, as shown in Fig. 2A. Vaz Jr *et al.* used hydroxymethylation to increase the surface area, adsorption, and availability of chemical groups for the interaction of the depolymerized kraft lignin components.[25] Amination adds amine functional groups to the lignin derivatives.[26] The Mannich reaction is one method to facilitate the amination of lignin. Jiao *et al.* investigated this approach by incorporating a phenolation pretreatment, producing aminated lignin with elevated nitrogen content and a low C/N ratio under ideal conditions.[27] Eraghi *et al.* have conducted amination of lignin in an alkaline environment using NaOH to synthesize cationic lignin.[28] Sulfomethylation of lignin adds methylene sulfonate groups to lignin with sodium sulfite and formaldehyde, producing sulfonated polyphenols, like sulfomethylated tannic acids.[29] Sulfonating lignin alters its charge density, solubility, and molecular weight, enhancing its potential for applications in surface modification, adsorption onto surfaces like kaolinite, and environmental remediation as a coagulant for dye removal. For example, Gao *et al.* conducted hydroxymethylation of kraft lignin by exposing it to a formaldehyde solution, yielding H-lignin. Subsequently, sulfonation was performed using sulfuric acid, resulting in a product with a charge density of 0.46 meq g^{-1} and 9% solubility. In contrast, employing Na_2SO_3 led to sulfonated lignin with a charge density of 1.2 meq g^{-1} and a complete solubility of 100%.[30] Using nitrating agents, such as nitric acid with acetic anhydride, acetic acid or sulfuric acid, nitration of lignin can be carried out.[26] Adding this modified lignin (1.4–6.0%) increases cross-linking density and, consequently, improves the mechanical properties of the final composites.[31]

Introducing new chemically active sites, such as amine, sulfonate, or hydroxyl groups, into lignin allows for better control of its properties, which enhances its suitability for the development of 3D printing materials. These modifications enable better control over lignin's reactivity, mechanical strength, and cross-linking density, making it adaptable in advanced additive manufacturing applications.

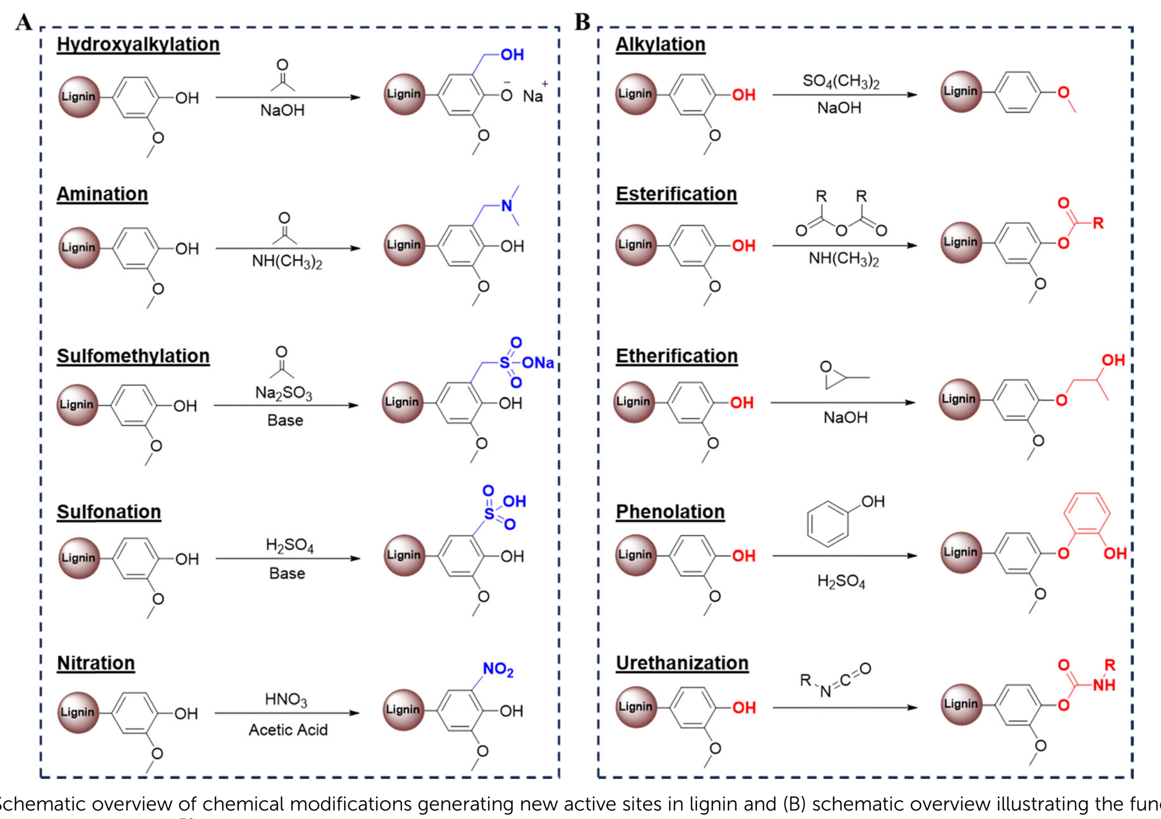

Fig. 2 (A) Schematic overview of chemical modifications generating new active sites in lignin and (B) schematic overview illustrating the functionalization of lignin's hydroxyl groups.[32] Copyright 2019, Elsevier.

2.2. Functionalizing hydroxyl groups

As previously mentioned, lignin possesses numerous phenolic and aliphatic hydroxyl groups, offering opportunities for functionalization to create highly reactive polyol derivatives useful across diverse applications. As shown in Fig. 2B, hydroxyl group modification can be achieved through alkylation, esterification, etherification, and phenolation. Jiang *et al.* explored alkylation with 1,6-dibromohexane, increasing lignin's molecular weight by 1643% and lightening its color significantly.[26] Zhang *et al.* showed the potential of lignin in 3D printing by synthesizing alkylated derivatives of dealkaline lignin (DAL) through a streamlined one-step esterification with undecanoyl and dodecanoyl chlorides, creating the modified forms DAL-11ene and DAL-12ane. These derivatives demonstrated significantly enhanced photoinitiation efficiency compared to unmodified DAL, with DAL-11ene's polymerizable group enabling direct integration into the polymer network. This modification promotes safe and effective use in 3D printing, as shown in successful digital light processing (DLP) under 405 nm exposure, marking a promising development for lignin-based photoinitiators in 3D printing.[33]

Esterification processes include ring-opening with cyclic esters, polymerization with carboxylic acid chloride, and dicarboxylic acids, as seen in butyl ester synthesis.[34] Dai *et al.* enhanced carbon nanofibers from organosolv lignin *via* esterification, improving the material's capacitance and stability.[35] Liu *et al.* developed a greener esterification method without catalysts or acyl chloride. In this method, kraft lignin was functionalized with organic acids, resulting in a polymer blend with a lower glass transition temperature suitable for 3D printing inks.[36] Deance *et al.* performed esterification of kraft lignin with methacrylic anhydride to incorporate into poly(ethylene glycol)diacrylate (PEGDA) matrices. The study demonstrates that methacrylated lignin can integrate smoothly within PEGDA, allowing properties like light shielding, mechanical strength, and antioxidant activity to be tailored in 3D-printed structures.[37]

Etherification methods such as polymerization with alkylene oxides or epichlorohydrin and solvolysis with ethylene glycol are effective in modifying lignin for increased monomer yield.[32] Dong *et al.* employed a diol pretreatment that enhanced α-etherification, minimizing ether bond cleavage and improving lignin isolation.[38] Cheng *et al.* confirmed similar improvements with a diol-based deep eutectic solvent.[39] Liu *et al.* developed a lignin-based macromolecular photoinitiator for 3D printing applications, introducing photoinitiating and water-soluble PEG groups into lignin. This lignin modification enables strong light absorption (200–400 nm), water solubility, and effective cross-linking when combined with glycidyl methacrylate-modified gelatin (Gel-GMA). The synthesized lignin-based photoinitiator improves biosafety, mechanical strength, and swelling control in hydrogels, showing lignin's promise as a biocompatible backbone for durable, ductile 3D-printed structures.[40]

Phenolation, involving lignin's reaction with phenol under acidic conditions, raises its phenolic hydroxyl content. Zhang *et al.* achieved high phenolic content through phenolation with pyrogallol in acetone and sulfuric acid.[41] Urethanization of lignin involves the formation of a urethane link between lignin hydroxyl groups and isocyanate groups.[42] This can be done by reacting lignin with diisocyanate and/or diol or by reacting isocyanate and polyol and then polymerizing with lignin.[43] Urethanization, linking hydroxyl and isocyanate groups, can be achieved with diisocyanates and polyols, as demonstrated by Lerma *et al.* with 4,4-methylene bis(phenyl isocyanate).[44] Advancing lignin-based 3D printing materials will require more targeted research on modifications of the hydroxyl group in lignin, such as alkylation, esterification, and urethanization, to enhance its reactivity and adaptability.

2.3. Lignin copolymers

Due to its abundance, cost-effectiveness, and minimal interference with food supplies, lignin is a pivotal resource for sustainable synthetic polymers. Yet, its complex structure and natural chemical inertness require specific modifications to realize its potential fully. Graft copolymerization, an effective method for lignin polymerization, introduces new functionalities that enhance its adaptability. This process not only expands lignin's utility across various applications, but it is potentially also valuable for the development of novel 3D printing materials, as it improves material homogeneity, printability, sustainability, and mechanical properties. Phenolic and aliphatic hydroxyl groups are ubiquitous in various types of lignin, offering reactive sites for incorporating diverse chemical groups into the molecular chains. These functional hydroxyl groups, as highlighted earlier, facilitate diverse reactions like alkylation, esterification, and amination.[45] Moreover, lignin is a potential macromonomer capable of hosting heterogeneous molecular chains. Notably, living polymerization techniques such as atom transfer radical polymerization (ATRP),[45–47] reversible addition–fragmentation chain transfer polymerization (RAFT),[48–50] ring-opening polymerization (ROP),[2,51] and formation of lignin polyurethanes[52–55] have been effectively utilized to synthesize lignin graft copolymers, offering a pathway to engineering lignin's chemical structure for enhanced functionalities. Deeper research on lignin-based copolymers opens new possibilities for developing 3D printing lignin materials. By leveraging the reactive sites on lignin's phenolic and aliphatic hydroxyl groups and employing advanced polymerization techniques, it is possible to tailor lignin's structure through copolymerization, which can form new materials with tunable properties, enhanced mechanical performance, and smart materials that are compatible with 3D printing processes, providing sustainable alternatives to petroleum-derived polymers.

3. 3D printing techniques used for lignin materials

From previous work on 3D-printed lignin materials, fused deposition modeling (FDM), stereolithography (SLA), and direct ink writing (DIW) are commonly adopted. A few works are on

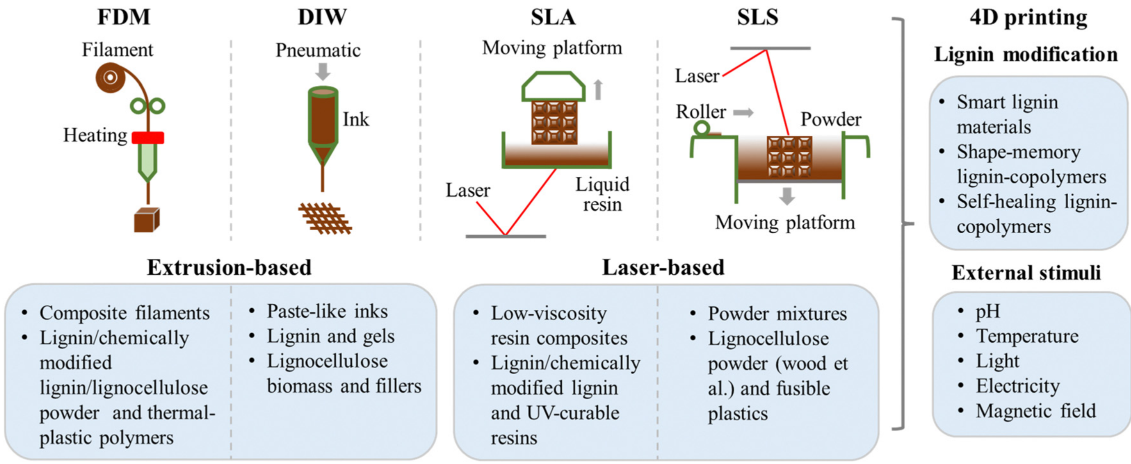

Fig. 3 Scheme of different 3D printing techniques used for lignin-based materials and derived 4D printing of lignin materials. Material extrusion: FDM and DIW; laser-based: SLA and SLS.

selective laser sintering (SLS) of lignin materials. FDM and DIW are extrusion-based printing techniques. The former involves the thermal extrusion of lignin and thermal plastic composite filaments, and the latter involves the extrusion of water-based paste-like inks of lignin/lignocellulose and other fillers. SLA involves light-curable materials, such as chemically modified lignin for UV curing properties and commercially available resins, where lignin is mainly used as an additive, and the matrix is a UV-curable resin. The primary benefit of adding lignin to the UV-curable resin system is partially replacing the fossil-derived resin with renewable bio-sourced lignin. As for the SLS, the lignocellulose biomass (wood powder, *etc.*) was mixed with fusible plastic powders for 3D processing. The majority of research has focused on the FDM of lignin-based materials, with significantly fewer studies reported on SLS. SLS appears to be less suitable for 3D printing lignin materials, as it primarily depends on the functionality of auxiliary polymers. Consequently, this section places greater emphasis on FDM, SLA, and DIW, while SLA is discussed in less detail. The scheme of these four different 3D printing techniques used for lignin materials and derived 4D printing of lignin materials is shown in Fig. 3.

For FDM, the chemical modification of lignin significantly enhanced the overall properties, particularly the mechanical performance, of 3D-printed lignin-based composites. In the case of SLA, the chemical modification of lignin notably increased its incorporation into resin composites, likely due to the enhanced interfacial interaction between the modified lignin and the resins. For DIW, higher lignin content is incorporated into the inks than other 3D printing techniques, and chemical modification is not deemed necessary. As for SLS, only wood flour is used in combination with other polymers, and lignin does not play a major role in the 3D printing process. The representative works discussed in this review are summarized in Table 1.

3.1. Fused deposition modeling (FDM)

Fused deposition modeling (FDM), also known as fused filament fabrication (FFF), is a commonly used 3D printing method, where 3D objects are built by depositing melted materials according to sectional geometry layer-by-layer. Specifically, the thermoplastic filament is loaded into the printer and extruded through a heated nozzle. The extrusion head can move along the X and Y axes to deposit the material in a predetermined pattern. The deposited material will then cool and solidify. Once the layer is printed, the platform lowers itself, or the nozzle head moves upwards to allow the deposition of the next layer until the object is finished.[73,74]

3.1.1. Direct blending/compounding of raw lignin for FDM. An ideal material candidate for FDM should fulfill specific rheology and thermal criteria. The material needs to have a low enough melt viscosity to facilitate extrusion. Yet, the zero-shear viscosity should be high enough so that the printed objects can stand freely without any dimensional changes. In addition, the material needs to have high mechanical properties to avoid buckling the filaments during printing and high thermal stability as heating is applied during extrusion in FDM.[75]

As the incorporation of lignin can alter the rheology and thermal properties of the polymer matrix, which can affect the processability and printability of such filaments, it is essential to define "printing zones", where key parameters such as viscosity and extrusion rates that can provide appropriate printing conditions for FDM are identified.[76] Ideally, lignin-containing composites should form a rigid system with stable melt to meet the criteria for smooth 3D printing *via* FDM. The situation is complicated by the variability in lignin structure depending on the sources and extraction methods. For example, Nguyen *et al.* studied the rheology properties of two types of lignin: kraft softwood (SF) lignin and organosolv hardwood (HW) lignin. HW lignin is sinapyl alcohol-rich and printable with low melt viscosity and high stiffness at room temperature. In contrast, SW lignin is coniferyl alcohol-rich and unsuitable for melt processing due to its high melt viscosity and high resistance to flow unless a low lignin fraction was used.[17,76] Obielodan *et al.* reported that the mechanical and thermal properties of 3D-printed objects from PLA/lignin composites varied significantly depending on the source of lignin used.[77]

Table 1 Summary of representative 3D/4D printing techniques used for lignin and lignocellulose materials

Source of lignin	Modification of lignin	3D printing technique	Polymer and additive	Lignin content	Application/results	Ref.
Kraft lignin	Unmodified	FDM	PLA and castor oil	0–3 wt%	Showing antioxidant capabilities; 3D-printed meshes show advantages in wound healing applications	15
Organosolv lignin	Unmodified	FDM	PLA, polyethylene glycol (PEG) 2000 and struktol TR451	Up to 20 wt%	The composite filaments show degraded tensile properties; when lignin content is above 25 wt%, filaments are brittle and do not have enough flexibility to be rolled in a filament spool	16
Enzymatic lignin	Unmodified	FDM	Polyhydroxybutyrate (PHB)	Up to 20 wt%	Lignin acting as a non-reactive filler; lignin affects the shear thinning profile, which helps in the layer adhesion in 3D printing and reduces the warpage of 3D printed samples compared to neat PHB	17
Organosolv lignin	Demethylation	FDM	Polyamide 12 (PA12)	10 wt%	Enhanced mechanical properties; a tensile strength of 46.1 MPa (40.2 MPa of PA12); improved anti-aging performance	56
Alkali lignin	Acetylated and hexanoated lignin	FDM	PLA	Up to 50%	Enhanced thermal stability and compatibility with PLA; mechanical properties are in the same range as pure PLA. Acetylated lignin showed UV-shielding and antioxidant properties compared to the 3D-printed composites	57
Alkali lignin	Enzymatically modified lignin	FDM	PLA and thermoplastic polyurethane (PU)	Up to 5 wt%	Partially degraded lignin used as a nucleating agent for PLA/PU blends; the matrix is PLA: PU (90 : 10); increased the elasticity modulus to a maximum of 2.5-fold; a maximum biodegradability rate of 15% after 6 months under the soil burial	58
Industrial lignin	Lignin nanospheres	FDM	PLA	0.5 wt%	Lignin nanospheres were prepared without changing the chemical structure of lignin; flexural, tensile, and impact strength increased by 130.8%, 56.1% and 14.2%; hydrogen bond action between lignin nanospheres and PLA	59
Wood flour	Unmodified	FDM	PLA	20 wt%	Ball-milled wood flour as reinforcement in PLA; 210 °C filament extrusion temperature and 230 °C printing temperature; particle size of wood flour negatively correlates with tensile strength	60
Kraft lignin	Unmodified	SLA	Photoreactive methacrylate resins	1 wt%	Lignin-based composite shows increased tensile strength by 46–64% and Young's modulus by 13–37%	61
Lignin-coated cellulose nanocrystal (L-CNC)	Unmodified	SLA	Methacrylate resin	Up to 1 wt% L-CNC	Post-curing induced interactions between the L-CNC and resin through the esterification reactions between methacrylate resin and –OH groups of L-CNC; enhanced tensile strength and thermal stability; reduced glass transition temperature	62
Organosolv lignin	Acylation	SLA	Urethane acrylate (Genomer 1122), tetraacrylate oligomer (SR494), and aliphatic urethane acrylate (Ebecryl 8210)	Up to 15 wt%	Photoactive acrylate resins for SLA by mixing commercial resin components with acylated organosolv lignin; a 4-fold increase in ductility with higher lignin concentration but decreased thermal stability	20
Organosolv lignin	Acylation and decolorization	SLA	Tetrahydrofurfuryl acrylate (THFA), pentaerythritol tetraacrylate (PETA), and diphenyl(2,4,6-trimethylbenzoyl)phosphine oxide (TPO)	40 wt%	Lignin is decolorized by acetylation and subsequent UV irradiation, reducing the UV absorbance by 71%; a 3D printing resolution of 250 μm; the stiffness and strength of 3D-printed composites increased by factors of 15 and 2.3	63
Kraft lignin	Lignin nanoparticles	DLP	Methacrylated eugenol (ME), methacrylated vanillin (MV) and methacrylated vanillyl alcohol (MVA)	Up to 2 wt% lignin nanoparticles	Lignin-derivable resin formulations; lignin acting as a UV absorber for better control of the photopolymerization process; improved the ductility of the 3D printed nanocomposites through toughening mechanisms enabled by the rigid lignin nanoparticles	64
Cork powder	Unmodified	SLA	Commercial photocurable resin: Form Clear v2	5 wt%	Cork in commercial resin; as the particle size of cork decreases, both the mechanical and thermal resistance increase	65
Alkali lignin	Unmodified	DIW	Pluronic F127	~60 wt%	Lignin and polymers in aqueous ink; lignin ratio of 18–32 wt%; triblock copolymer Pluronic F127 as the crosslinking agent to improve the rheological and viscoelastic properties of the inks; improved stability in water and under heat compared to cellulose, and UV-blocking performance; activated carbon from a 3D-printed lignin scaffold for water treatment	66

Table 1 (continued)

Source of lignin	Modification of lignin	3D printing technique	Polymer and additive	Lignin content	Application/results	Ref.
Organosolv lignin	Unmodified	DIW	Tempo-oxidized CNF (TOCN) and cellulose nanocrystals (CNC)	~25 wt%	The ink components can all be extracted from waste wood; freeze-drying and hot-press to densify the 3D-printed materials; mechanical properties are close to those of natural wood	67
Unbleached pulp	TEMPO-mediated oxidation and ultrasonication treatment	DIW	No	26.7% lignin in the unbleached pulp	2,2,6,6-tetramethylpiperidine-1-oxyl (TEMPO)-mediated oxidation and ultrasonication approach to process the pulp into lignocellulose nanofibrils; LCNF as a viscoelastic gelatinous ink for DIW; 3D-printed aerogels for customizable thermal insulation	68
Wood flour	Unmodified	DIW	Xyloglucan and cellulose nanocrystals (CNC)	~97 wt%	Directly mixing at various ratios; 100% wood-based materials; predesigned and programmed warped geometry by adjusting 3D printing pathways and printing flow rates	69
Alkali lignin	Unmodified	SLS	Polyamide (PA12)	Up to 60 vol %	30% less degradation at elevated temperatures than pure PA12; a higher porosity (~10%), increased Young's modulus by ~16%, and reduced tensile strength by ~7%; reduced cost	70
Enzymatic lignin	Unmodified	4D printing (FDM)	PLA, polyamide elastomer (PAE, PEBAX 2533)	Up to 3 wt%	Lignin acting as the photothermal conversion module; initiating and controlling the shape memory under near-infrared (808 nm) laser irradiation; enhanced toughness by lignin addition	71
Kraft lignin	Complexation with protein	4D printing (FDM and DIW)	Keratin, PEG-400, guar gum	Up to 19 wt%	Keratin-lignin (ratio 4 : 1) for compounding and filament extrusion; two biopolymer systems; complexation of keratin and lignin through keratin amido and lignin aryl hydroxyl interactions; mechanical response to moisture stimuli	72

Moreover, increasing lignin in the composites is often accompanied by deterioration of their mechanical performance. Various studies have reported a reduction in the mechanical properties of the composites when lignin is added to polymers.[16,78–81] This was explained by a decrease in the effective load-bearing area of the polymer in the presence of lignin.[82] Due to poor compatibility and interfacial interaction between lignin and the polymer, aggregation of lignin particles occurs at high content, leading to a smaller interfacial area, resulting in poor stress transfer between the polymer and lignin. The poor mechanical properties of lignin-containing composites affect the overall mechanical performance of final 3D-printed objects.

The choice of polymer in lignin-containing composites is another critical consideration, where PLA and ABS are the most commonly used polymers. Many studies have reported decent printability of lignin-containing composites based on PLA. However, mechanical properties are often compromised with lignin addition compared to those with neat polymers. Tanase-Opedal *et al.* reported that adding soda pulping lignin at 20 and 40 wt% to PLA reduced tensile strength, elastic modulus, and strain at break of FDM 3D-printed objects. However, adjusting printing temperatures could alleviate this reduction in tensile strength.[19] Weakening of 3D-printed objects with lignin composites was also observed by Mimini *et al.*, where both impact and flexural strength of lignin/PLA composites decreased with increasing lignin content up to 15 wt% for three types of lignin (kraft lignin, organosolv lignin, and lignosulfonate).[83] The reduction in flexural strength was attributed to the disruption of interactions between PLA chains, while the decrease in impact strength was explained by the high rigidity of lignin and the presence of voids in the composites, potentially introducing flaws into the structure. Gkartzou *et al.* reported that tensile strength and elongation at break were lower for 3D-printed objects using lignin/PLA composites at 5% loading than pure PLA objects.[84] This was explained by the better interlayer fusion in pure PLA objects. The interlayer fusion was improved every two layers due to toolpath variation in pure PLA objects, which was not evident in lignin/PLA objects.

To mitigate the issue of poor mechanical performance, researchers have tried to add other components to improve compatibility between lignin and polymers. Ren *et al.* were able to achieve a high lignin loading of 50% in lignin/PLA composites with good printability by adding plasticizers (acetyl tributyl citrate and tributyl citrate), which enhanced lignin dispersion and polymer chain mobility. The integration between printed layers was also increased because of higher local chain relaxation.[85] Wasti *et al.* tried using PEG and struktol TR451 as plasticizers in lignin/PLA composites. Although mechanical strength was improved with plasticizer addition, the tensile strength of 3D-printed objects with 20% lignin content was still lower than that of pure PLA.[16] The addition of epoxidized palm oil (EPO) was shown to be less effective in enhancing the mechanical properties of lignin/PLA. Even with EPO addition, the mechanical properties of lignin-containing composites started to decrease and were lower than those of neat PLA once the lignin content exceeded 3%.[86]

For lignin/acrylonitrile-butadiene-styrene (ABS) composites, the addition of lignin often resulted in more brittle materials, where the tensile strength and strain at break were significantly reduced from pristine ABS when organosolv HW lignin was added at 40 wt%.[87] The same group then incorporated acrylonitrile butadiene rubber (NBR41, 41 mol% nitrile content) to improve the plasticity of the lignin/ABS composite. Adding 10 wt% rubber to lignin/ABS composites remarkably increased the tensile strength and strain at break, making the materials much more printable.[88] The mechanical properties and printability were further enhanced by adding 10 wt% carbon fiber (CF). The percolation of CF reinforced the polymer matrix and contributed to the increased mechanical properties of the composites. The welding between layers was significantly stronger when CF was added, as seen in Fig. 4A. The SEM images indicated unfused regions between two layers for neat ABS and ABS composites containing lignin and rubber, as highlighted with yellow arrows (Fig. 4B). This issue was not observed when CF was added to the composites. The enhanced fusion between layers was due to higher local chain mobility, thus lowering local melt viscosity as CF disrupted crosslinking between lignin and rubber.[88] Additionally, imperfect alignment of CF orientated towards the weld interface formed CF bridges, reinforcing the interlayer welding. The 3D-printed objects are demonstrated in Fig. 4C. Moreover, adding polyethylene oxide (PEO) to lignin/ABS served similar purposes as nitrile rubber since PEO acted as an adhesion promoter and helped the dispersion of lignin in the ABS matrix (Fig. 4D).[89] The addition of graphene to ABS/lignin composites could also enhance their mechanical properties, which allowed successful 3D printing of complex shapes (Fig. 4E). However, the surface finish was

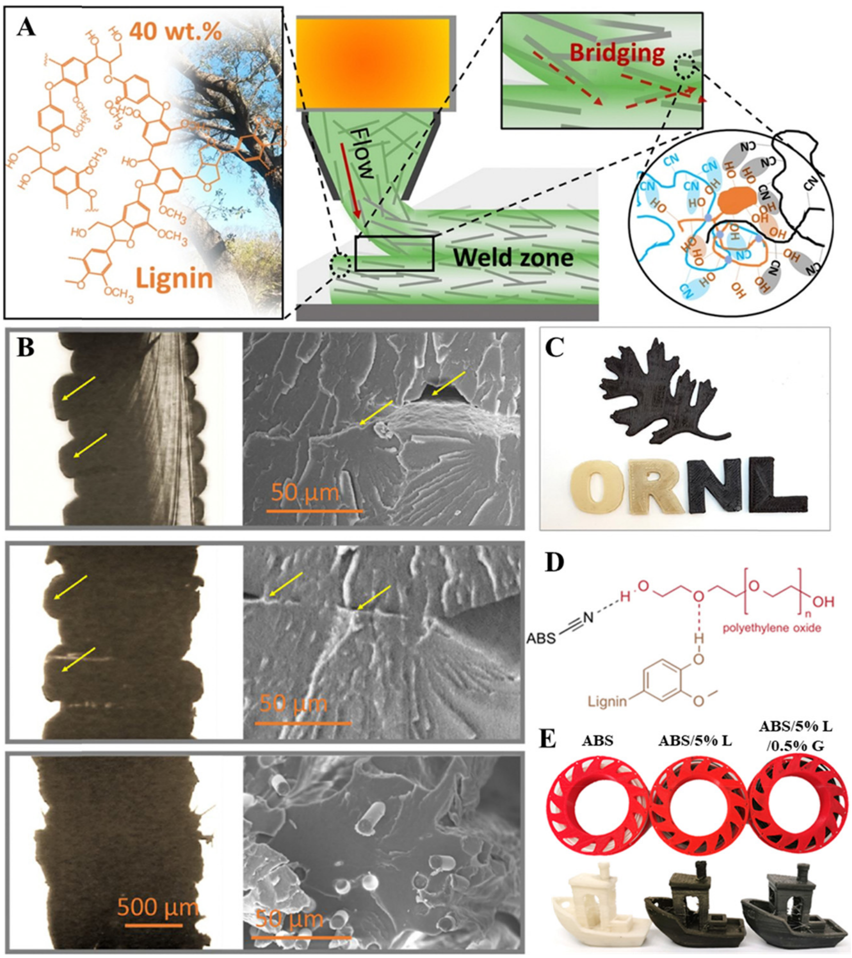

Fig. 4 (A) Scheme to highlight the alignment of CF along the printing flow and CF bridging the weld zone.[88] Copyright 2018, Elsevier. (B) The cross-section optical images (left) and corresponding cross-section SEM images (right) of the 3D-printed samples: (top) ABS; (middle) ABS-NBR41-Lignin-514; and (bottom) ABS-NBR41-Lignin-CF-4141. The yellow arrows in the optical images (left) and in the SEM images (right), top and middle, indicate individual 3D-printed layers and unfused areas, respectively. (For interpretation of the references to color in this figure legend, the reader is referred to the web version of this article.).[88] Copyright 2018, Elsevier. (C) Examples of 3D-printed objects made from ABS ("O" and "R"), ABS-NBR41-Lignin-514 ("N"), and ABS-NBR41-Lignin-CF-4141 ("L" and the oak leaf).[88] Copyright 2018, Elsevier. (D) The hydrogen-bonded network of lignin with PEO in the ABS matrix.[89] Copyright 2015, American Chemical Society. (E) The filament rolls at different composition ratios of ABS, lignin (L), and graphene (G); the quality of 3D printed objects.[90] Copyright 2021, Wiley-VCH.

affected, and the added lignin content was only 5% before tensile strength started to fall.[90]

Other polymers have been studied for their utilization in FDM of lignin-based composites. Nguyen *et al.* attempted to develop printable nylon/lignin composites. They found that adding HW lignin increased the stiffness of the composite at room temperature and reduced its melt viscosity, leading to excellent 3D printability. This was explained by the phase-separated discrete lignin domains forming thermos-reversible hydrogen bonding with the nylon matrix.[76] In this case, the addition of CF also further increased the material tensile strength and reduced the melting temperature of the polymer matrix, allowing printing with a higher rate and lower temperature. Zhou *et al.* fabricated polyurethane/lignin composites with good rheology behavior suitable for printing up to 50 wt% lignin. However, tensile strength and elongation at break were not ideal with lignin addition. This issue was alleviated by adding 0.5 wt% carbon fibers, which reinforced the mechanical properties and increased interlayer bonding during 3D printing.[91] Vaidya *et al.* reported that although the surface part quality and warpage were improved for a lignin/polyhydroxy butyrate (PHB) composite at 20 wt% lignin (biorefinery lignin), increasing the lignin content to 50% renders the composite unsuitable for FDM, due to increase in required pressure to print.[17] The decrease in warpage was explained by the interfacial voids in the composites, as the voids modified the volume shrinkage behavior. The interfacial voids in lignin/PHB composites resulted from incompatible interfaces between lignin and PHB. Yu *et al.* fabricated lignin/PEO composite filaments for 3D printing and found that filaments containing HW lignin with 15 wt% PEO showed thermal and mechanical properties suitable for FDM.[92]

Attempts have been made to form composites with other polymers, but with less promising results. For example, combining lignin and nitrile rubber resulted in composites with excellent mechanical properties but were very difficult to print due to the high viscosity. This may be mitigated by blending further with rigid plastics.[14] Extrudable FDM filaments could be made by mixing keratin and lignin at a temperature higher than 130 °C. However, degradation of composites was observed at such high temperatures.[72]

3.1.2. Modified lignin and lignin copolymers for FDM. Chemically modified lignin and lignin-based copolymers have been developed to overcome the poor mechanical properties of lignin/polymer composites. It is now recognized that poor dispersion and interfacial interaction between lignin and the polymer matrix cause the suboptimal mechanical performance of lignin-containing composites. Therefore, efforts have been made to improve the compatibility and dispersion of lignin in the polymer matrix, either by changing lignin chemistry or morphology.

Yao *et al.* reported that by using acetylated lignin and hexanoated lignin, good mechanical properties and printability could be achieved for lignin/PLA composites having up to 50% lignin content, with mechanical properties in the same range as pure PLA.[57] Gordobil *et al.* also reported that when acetylated lignin was used to form composites with PLA, elongation at break was increased even at high acetylated lignin content.[79] Hong *et al.* modified the lignin surface by adding hydroxyl groups. The tensile strength of composites consisting of PLA and modified lignin was increased from that of PLA/non-modified lignin composites. Successful 3D printing of PLA composites with modified lignin was demonstrated up to a lignin content of 15%, above which the binding between printed layers became difficult.[93] Zhang *et al.* used a demethylation method to enrich the phenolic hydroxyl groups on organosolv HW lignin. By adding modified lignin at 10 wt%, tensile strength, Young's modulus, and anti-aging performance of 3D-printed objects were improved compared to objects printed from nylon 12 alone. The improved mechanical properties were attributed to better interfacial interaction between lignin and the nylon matrix, as the added hydroxy groups provided potential hydrogen bonding sites.[94] Liu *et al.* added lignin treated with a silane agent (KH550) to PLA, which improved the mechanical properties of composite filaments compared to neat PLA. Tensile strength remained higher than neat PLA, up to a lignin content of 20%. When lignin content exceeded 20%, poor dispersion of lignin in the PLA matrix was observed, which resulted in reduced tensile strength.[95] Ye *et al.* developed a customized compatibilizer containing lignin and PLA moieties, lignin-*g*-maleic anhydride-*g*-PLA (LMP), for a 3D printable lignin/PLA composite. By adding this compatibilizer to lignin/PLA composites, molecular interaction, and mechanical properties were significantly improved.[96]

Biological treatment can be applied to modify lignin chemistry as well. Murillo-Morales *et al.* used an enzyme, bacterial laccase, to partially degrade alkali lignin before adding it to a polymer blend of PLA and thermoplastic polyurethane. During degradation, various chemical reactions occurred, and the surface area of lignin increased significantly. These changes allowed better compatibility between lignin and the polymer matrix. The resultant composites had improved tensile strength, Young's modulus at low lignin content (up to 5%), and good printability. The printed parts containing enzyme-degraded lignin at 5% lignin content had superior biodegradability (15 wt% weight loss after six months) compared to the polymer blend alone.[97]

Sun *et al.* synthesized lignin-poly(D-lactide) (PDLA) copolymers and lignin-rubber-PDLA copolymers, which were then added to poly(L-lactide) (PLLA) to form composites.[98] It was found that composites with both copolymers showed higher tensile strength, Young's modulus, elongation at break, and toughness compared to pure PLLA polymers due to stereo-complexation between PDLA and PLLA, which promoted load transfer from the matrix to lignin copolymer filler. The addition of rubber further enhanced toughness and elongation at break, as rubber could initiate crazing under stress. Ding *et al.* copolymerized 2-ethylhexyl acrylate with lignin (e-lignin) and reported that adding 10 wt% e-lignin to PLA significantly toughened the composites. The toughening effect was explained by plasticization and good interfacial compatibility between e-lignin and PLA. The composites showed good printability, and the interlayer adhesion for 3D-printed objects was improved due to the higher local relaxation of polymer chains.[99]

Other than chemical modification, physically modified lignin has also been studied. Long *et al.* prepared lignin nanospheres without changing the chemical structure of lignin. The lignin nanospheres were then compounded with PLA at 0.5 wt% to form composites with enhanced mechanical properties and good printability for FDM.[59] Similar results were obtained for lignin microspheres. The addition of 0.375 wt% lignin microspheres to PLA produced composites with enhanced tensile, bending, and impact strength. The composites were then successfully printed *via* FDM.[100]

3.1.3. Lignocellulose biomass for FDM. Various studies have explored using lignocellulose biomass to form composites for FDM instead of lignin extracted from biomass. Many different types of biomasses have been used for FDM, such as wood, bamboo, sugarcane, and hemp, to name a few. The composition of biomasses can vary remarkably between species and sources, implying different amounts of lignin. Therefore, different mechanical and thermal behaviors have been observed for 3D-printed objects containing different biomasses.[60]

Wood is one of the most used biomasses as a natural filler due to its low cost and wide availability. A considerable number of studies on this topic are available in the literature. Like lignin, the incorporation of wood often leads to decreased mechanical performance of 3D-printed objects, mainly due to the intrinsic poor tensile strength and brittleness of wood-containing composites and the high porosity induced during printing.[101–105] For example, Kariz *et al.* reported that the tensile strength of wood/PLA composites decreased after the wood particle content reached 10%. In addition, with increasing wood content, the printability became poorer, and 3D-printed objects became rougher and more porous.[101] The high porosity of 3D-printed objects using wood/PLA composites was also observed by Le Guigou *et al.*, which could be an advantage when the printed samples are developed into hygromorph materials.[102] Li *et al.* developed a bio-hygromorph with fish swim bladder hydrogel and a 3D-printed scaffold from wood/PLA composites. The morphing abilities could be triggered by changes in moisture content.[106] Various printing parameters were found to affect the mechanical strength, porosity, and wettability of the printed samples, including printing width,[102] printing temperature,[103] printing layer thickness,[107–109] printing pattern,[109] and the number of shells.[104] Other factors including the addition of plasticizers,[63] incorporation of compatibilizers and toughening agents,[64] chemical treatment of biomasses,[65] and wood particle size reduction[53] can potentially improve the mechanical performance and affect the wetting behavior.

Bamboo is another biomass that has been used extensively in FDM. The mechanical performance and microstructure of 3D-printed objects using bamboo-containing composites have been investigated, and factors affecting their mechanical performance include infill density and deposition geometry.[110–112] Chemical treatment has also been applied to bamboo, which improved the mechanical performance of 3D-printed objects.[113] Other types of biomasses have also been utilized in 3D printing, and some examples are provided here. Song *et al.* looked at composites containing PLA and walnut shells, containing around 30% lignin, and pre-treated with NaOH and the silane coupling agent (KH550). The composites were successfully 3D-printed into porous scaffolds with controllable porosity and pore size using FDM.[114] Liu *et al.* reported an increase in flexural modulus when sugarcane bagasse was used in PLA, and the printing orientation affected the tensile strength of 3D-printed objects due to the orientation of sugarcane fiber and polymer chains under different printing modes.[115] Yu *et al.* achieved the 3D printing of PLA and rice straw powder composites and found that the particle size, alkali, and ultrasonic treatments on rice straw powder could improve mechanical strength.[116] Ni *et al.* developed biocomposites of PLA, thermoplastic starch, and *Astragalus* residue powder for FDM. The inclusion of both biomasses decreased the mechanical properties of the composites.[117]

To summarize lignin materials for FDM, the mechanical strength of composites and 3D-printed objects tends to decrease when lignin or lignocellulose biomass is added, and these natural materials are directly blended with a polymer matrix. Since the main reason for poor mechanical performance is low compatibility between fillers and the matrix, different strategies have been developed to overcome this issue. Chemical modification and copolymerization have been demonstrated to effectively increase the interaction between the filler and matrix, thus improving mechanical performance. Additives that serve different purposes have been incorporated as well. For example, compatibilizers that can form hydrogen bonding with either or both components could effectively enhance filler–matrix interaction, which in turn enhances mechanical performance. Toughening agents achieved the same purpose by reinforcing the composite structure. In addition, defects introduced during printing, such as poor interlayer adhesion and high porosity, also contributed to inferior mechanical performance. Additives that can improve interlayer welding by plasticization of polymer chains or bridging effects have also been proven to be effective in enhancing the mechanical properties of 3D-printed objects.

Given these limitations, the use of lignin to replace petroleum-based polymers in FDM by direct blending is restricted by poor printability and mechanical performance at high lignin content. Currently, FDM has only been successful at relatively low lignin content. Proposed strategies to rectify these issues can cause further problems. For example, chemical modification can increase the process's carbon footprint, and the additives used are not necessarily natural material-based, therefore forgoing the purpose of lignin application in favor of greener and more sustainable materials.

3.2. Stereolithography (SLA)

Stereolithography (SLA) and digital light processing (DLP) are similar methods that use a power source such as UV or a laser beam at a specific wavelength to control the *in situ* polymerization of desired parts in a polymer matrix. Lower viscosities of the printing matrices in a resin bath are desirable for this purpose, specifically with Newtonian flow behavior.[20,118] The primary distinction between SLA and DLP relies on the polymerization steps, where SLA utilizes point-by-point curing by scanning across the resin surface, whereas DLP involves curing of a layer in an *X–Y* plane at once.[119] The structural fidelity of the final product depends on various factors such as penetration depth, critical energy requirement to induce polymerization, dosage per layer, exposure time, and filler size/loading.[64,118,120,121] The formulation of a printing bath typically contains photosensitive monomers, photoinitiators, UV-blockers (to prevent over-curing), and a viscosity modifier. The higher reliance on non-renewable feedstock has led to seeking the possible pathways of using bio-derivable natural sources. Given the attractive properties and complex chemistry of lignin structure, scientists have paved the way for utilizing this as a functional material in vat polymerization. Initially, lignin was primarily investigated for its potential as a filler material. However, over time, researchers have explored its versatility in various roles beyond filling. These include functioning as a monomeric material, UV blocker, and photoinitiator, with particular emphasis on its reinforcement effects. These aspects will be further examined in the following two subsections.

3.2.1. Direct blending/compounding of lignin for SLA. Zhang *et al.* utilized softwood kraft lignin at loadings below 1 wt% to probe the ability of lignin as a reinforcing filler in a methacrylate resin.[61] Here, an optimum loading of 0.4 wt% generated a tensile strength of 49.0 MPa with a 60% increase compared to the control sample without lignin. However, a higher lignin loading (1 wt%) led to a lower stiffness of the structure, mainly due to the high amount of unreacted resin in the structure. Additionally, the authors documented a clear improvement of the mechanical properties after the post-curing for 4 h of the final structure. In another study, Ibrahim *et al.* studied the reinforcing effect of organosolv lignin from oil palm empty fruit bunch fibers using graphene nanoplatelets.[122] Lignin loadings from 0.2 to 3.0 wt% were incorporated in a polyurethane-based resin in a DLP system, which enhanced the strength profile of the composite by 27%, while a loading of 0.6 wt% lignin and 10 wt% graphene nanoplatelets indicated a significant improvement by 238% compared to the unmodified polyurethane resin.

Another attempt was made to generate conductive composite materials (a conductivity of 1.6×10^{-7} S cm^{-1} at 1 wt% lignin) with acrylic resins and *para*-toluene sulfonic acid doped polyaniline-organosolv lignin (PTSA/PANI/Lignin) combined filler materials.[120] This work revealed that lignin below 3 wt% could be successfully 3D-printed by vat polymerization, whereas a lignin content of 1 wt% indicated minimal surface roughness, resulting in an improved visual appearance. The limitation of the low loading has been attributed to the UV absorption by lignin, which hinders the curing process by obstructing the photo-initiators. Yao *et al.* turned this inherent limitation into an advantage by employing lignin nanoparticles to act as UV absorbers. This strategy aimed to improve 3D printing resolution by hindering light penetration into unintended layers.[64] Here, lignin nanoparticles have been considered as functional fillers, which indicated better dispersion stability and improved the ductility of the cured nanocomposites (Fig. 5B(ii)). Additionally, the team utilized a bio-based resin for the printing, which consisted of methacrylated derivatives of vanillin, vanillin alcohol, and eugenol to feature soft and rigid domains in the printing materials. However, in all these cases, the lignin content incorporated into the final product was limited (less than 3 wt%). Further enhancements towards this have been attempted mainly by using chemical modifications on the lignin structure to improve the adhesion of lignin with the polymer matrix.

The primary focus of lignin chemical modification has been on functionalizing lignin using methacrylate derivatives, with the goal of improving curing properties with reduced UV energy dosage while simultaneously enhancing mechanical properties with higher lignin loadings. Sutton *et al.* reported that lignin acylation using methacrylic anhydride enabled the loading of 15 wt% in the printing resin.[20] Furthermore, this system indicated a four-fold increase in ductility with a better layer fusion and high visual clarity compared to the commercially available resin without modified lignin (Fig. 5B(iii)). In this context, the increased incorporation of altered lignin suggests its potential application as a UV blocker, albeit with reduced effectiveness compared to the commercially available one (PR 48). Another study conducted by the same team reported the improvement of UV curing properties of organosolv lignin-containing resins by adding a reduction step before the acylation to address this.[118] Here, the authors utilized $NaBH_4$ chemical reduction to decrease photoactive sites further for more controlled curing by increasing UV transparency. Moreover, a comparison between acylation performed through two methods involving methacrylic anhydride and acrylic anhydride was made. The acrylic anhydride-treated lignin samples exhibited shear-thinning characteristics, which proved unsuitable for SLA printing, where Newtonian behavior was desired. An optimum loading of 5 wt% for reduced and methacrylated lignin was suggested. In both the stated studies, increased strength and lower thermal stability compared to the base resin have been reported.[20,118] Deance *et al.* carried out a copolymerization reaction on methacrylated kraft lignin with poly(ethylene glycol)diacrylate (PEGDA) to study the effect of loading up to 10 w/v%.[37] An optimum loading of 5 w/v% methacrylated lignin has led to 15–20% higher stiffness, with improved resistance and fracture toughness (Fig. 5B(i)). Additionally, when considering the antioxidant activity of the cured samples, the authors reported that adding 0.5 w/v% lignin resulted in a 40% increase, reaching a maximum of 50% for subsequent loadings. Another study conducted by Johnson *et al.* utilized methacrylated dealkaline lignin (2.5 wt%) in a bio-based resin containing soybean oil and vanillin.[126] The self-healing capabilities of the composites at 140 °C (24 h) have been reported owing to the transesterification process of

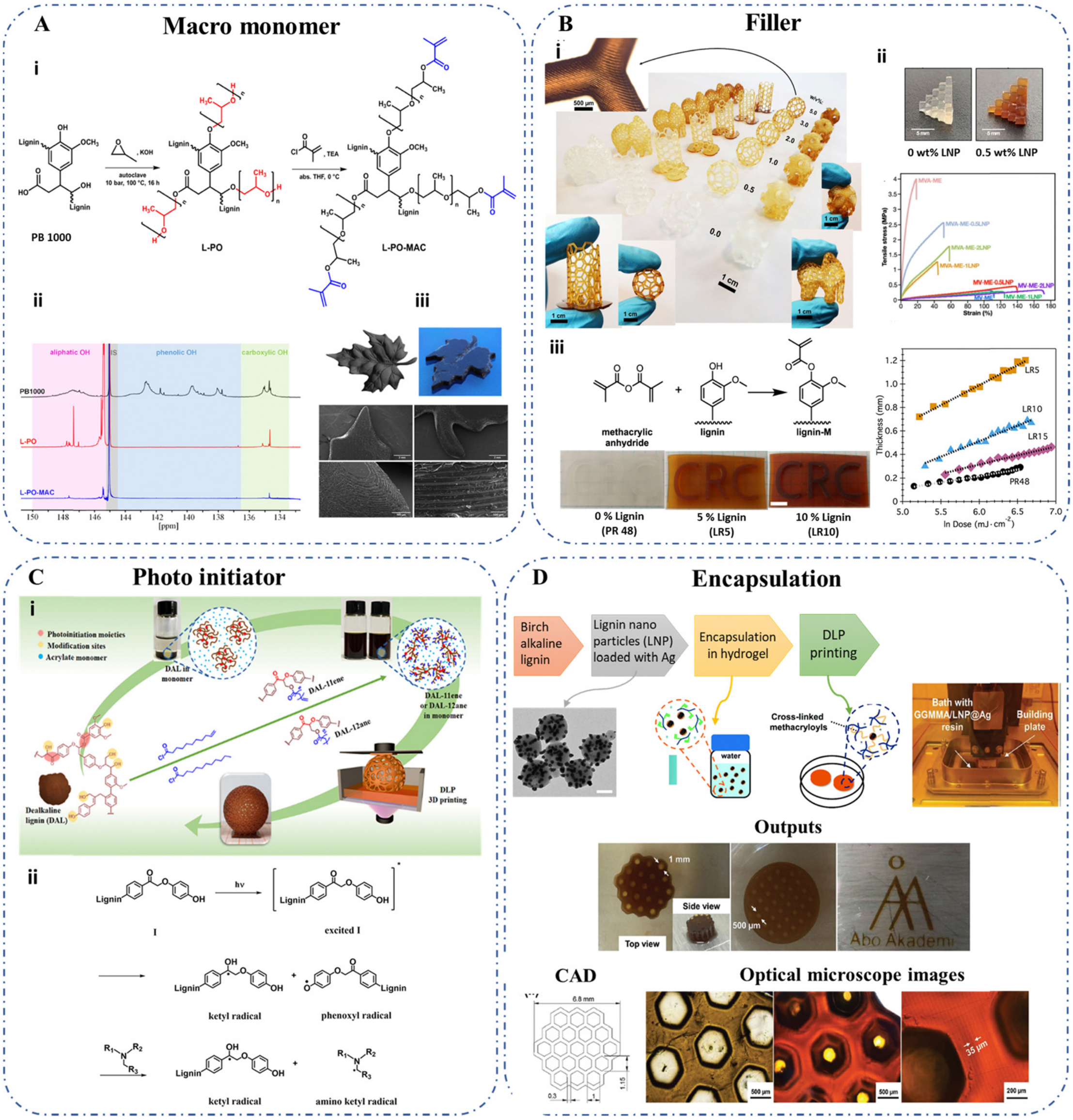

Fig. 5 Utilization of lignin for SLA and DLP 3D printing categorized by the function of lignin. (A) Lignin as a macromonomer: (i) modification pathway of wheat straw lignin to generate a photopolymerizable macromonomer. (ii) 31P-NMR spectra of wheat straw soda lignin (PB1000), propoxylated lignin (L-PO), and methacrylated propoxylated lignin (L-PO-MAC). (iii) CAD render, printed maple leaf and SEM images of the show parts.[123] Copyright 2023, American Chemical Society. (B) Lignin as a filler: (i) Photos of 3D printed composites with kraft lignin copolymerized with PEGDA at 0–5 w/v% (top left: optical microscope image of sample 5 w/v%,[37] Copyright 2023, American Chemical Society). (ii) Photos of lignin nanoparticle (LNP) incorporated specimens and stress–strain curves indicating tunable strength and ductility profiles at different LNP loadings (0.5–2.0 wt%), polymer matrix (MV: methacrylated vanillin; MVA: methacrylated vanillyl alcohol; ME: methacrylated eugenol),[64] Copyright 2023, Elsevier. (iii) Synthesis of methacrylated lignin and the effect of methacrylated lignin addition on the layer thickness and print quality; scale bar is 1 cm.[20] Copyright 2018, American Chemical Society. (C) Lignin as a photoinitiator: (i) grafting long alkane (DAL-12ane) and alkene (DAL-11ene) chains, (ii) generation of free radicals in dealkaline lignin under light.[124] Copyright 2020, American Chemical Society. (D) Lignin for encapsulation: silver-lignin nanosphere generation for encapsulation in the hydrogel for DLP printing.[125] Copyright 2022, The Royal Society of Chemistry.

methacrylated lignin due to the abundant hydroxyl and ester groups within the structure in the presence of a 2 wt% zinc catalyst.

Recently, Keck *et al.* explored a different avenue in an attempt to convert wheat straw lignin to a photopolymerizable macromonomer rather than utilizing lignin as a filler.[123] The team introduced a UV-curable lignin derivative with over 30% lignin content by an oxyalkylation reaction followed by a modification with methacryloyl chloride (Fig. 5A). Here, hot lithography was used to enable the processing of resins with high viscosity (up to 20 Pa s) at elevated temperatures. The as-printed structures exhibited a tensile strength of 13.5 MPa and Young's modulus of 220 MPa. Furthermore, the authors emphasized the significance of appropriately choosing the photoinitiator and its quantity, as this decision can impact the rheological properties of the resin system prior to crosslinking. The grafting of 90% hydroxyl groups in the lignin structure has enabled this macromonomer to be used as the resin without diluents (Fig. 5A(ii)). In another study, Zhang *et al.* probed the ability of lignin to act as a macro photoinitiator using dealkaline lignin.[124] The resin solubility was enhanced by introducing long alkane (DAL-12ane) or alkene (DAL-11ene) groups into the backbone, and the combination of an amine co-initiator [ethyl 4-(dimethylamino)benzoate] improved the photoinitiation efficiencies in DLP-based printing at 405 nm (Fig. 5C). The authors highlighted that even though dealkaline lignin has a certain level of photoinitiation ability, this modification enhanced the efficiency of acrylate monomers. Furthermore, the lower migration levels of these macroinitiators have confirmed the cytocompatibility of the polymer products.

Besides chemically modifying lignin to facilitate its incorporation, decolorizing lignin is another approach to avoiding its light absorption. In recent work, dark brown lignin was decolorized by UV irradiation to eliminate its UV absorption, resulting in a much higher lignin content of up to 40 wt% in the composites for DLP 3D printing.[63] Lignin was decolorized by acetylation and UV irradiation, reducing the UV absorbance by 71% after decolorization. The decolorized lignin incorporated into bio-based tetrahydrofurfuryl acrylate could work as a reinforcing agent for the 3D-printed objects, leading to increased stiffness and strength by factors of 15 and 2.3, respectively.

The generation of lignin nanoparticles, which are embedded with silver nanoparticles on the surface as antimicrobial agents, has been studied by Wang *et al.*[125] DLP printing at 405 nm has been utilized to print methacrylated *O*-acetyl-galactoglucomannan (GGMMA) hydrogels containing these lignin nanoparticles. Nanoparticle preparation with birch alkaline lignin was initially conducted by treating with three alcohols (isopropyl alcohol, ethanol, and methanol, respectively) to obtain well-defined lignin fractures, followed by a laccase-catalyzed polymerization step. The laccase-based polymerization has led to the generation of alkali-resistant lignin nanoparticles, which has enabled the *in-situ* reduction of Ag^+ with the possibility of loading 30.6–47.2 wt% silver nanoparticles. 3D-printed structures with 1 mm pore size and 35 μm layer thickness could be achieved in the printing process (Fig. 5D).

The incorporation of lignin with other biomasses is encouraged to improve overall properties such as reinforcement, hydrophobicity, and thermal stability of the final composites. Feng *et al.* studied the effects of reinforcement and thermal stabilization attained by incorporating 0.1, 0.5, and 1 wt% lignin-coated cellulose nanocrystals (L-CNC) in methacrylate composites.[127] The L-CNC utilized in this study contained 3–6 wt% lignin. The effect of post-curing (40 min at 120 °C) indicated enhancement of the properties of the composites owing to the esterification reactions, which occurred between methacrylate resin and the free –OH groups of the L-CNC. Compared to the neat resin, an improvement in tensile strength ($\sim$36.6 MPa at 0.5 wt% loading) and reduction of glass transition temperature with the increase in L-CNC loadings indicated the restriction of the chain mobility of the polymer matrix leading to better reinforcement and less energy consumption during the SLA 3D printing process. Later, the same team suggested the advantages of incorporating lignin-coated cellulose nanofibers (L-CNF) for energy saving with respect to post-curing.[128] Here, without performing any post-curing step, the team compared the mechanical properties of 3D-printed composites with L-CNF. The mechanical interlocking network with the matrix generated by the L-CNF resulted in the reinforcement of approximately 36.5 MPa at a much lower loading level (0.1 wt%). However, in both these studies, loading at 1 wt% indicated agglomeration of the particles.

3.2.2. Lignocellulose biomass for SLA. The effect of the particle sizes of lignocellulose biomass has also been studied.[65,121] The biomasses (wheat straw, rice straw, and cork powder) with sizes ranging from 45 to 250 μm have been incorporated into commercially available resins at 5 wt%. The thermal analysis of wheat straw and rice straw incorporated composites indicated better thermal stability owing to the high amounts of lignin present in larger particles.[121] Zhang *et al.* reported the enhancement of the strength profile of wood flour-reinforced (1–2 wt%) methacrylate composites.[129] At 1 wt% loading, the tensile strength increased to 24.7 MPa with respect to the neat polymer (21.1 MPa). A reduction in the glass transition temperature has been observed with higher wood powder loadings, attributed to increased free space occupied by polymer chains. Additionally, the team reported a stress whitening behavior (an energy-absorbing mechanism of plastic-type materials) of the composite materials owing to the formation of micro-craze and micro-voids, indicating the ability of wood flour to create localized stress points. A similar observation of stress whitening was evidenced by Yao and Hakkarainen.[130] Here, the authors were able to generate stable composites (617% increase in tensile strength compared to the neat polymer) with higher wood fiber loadings at 10 wt% in methacrylated eugenol and vanillin-based resin. A rapid functionalization of the wood fiber with microwave treatment has been reported here with enhanced interfacial adhesion. The authors attributed this to the generation of crosslinks between methacrylated wood fiber and resin. Additionally, an improved print fidelity has been observed in the wood powder incorporated composites as opposed to the control polymer without. The authors also reported a sedimentation of the filler at loadings above 10 wt%.

Overall, all these directives suggest the possibility and greater potential of lignin to have various roles in vat polymerization-based 3D printing. However, the careful selection and balancing of lignin chemistry are required to harness the fullest potential of this renewable source. Especially, the availability of convertible moieties enables researchers to delve more into the possible functionalization and modifications of lignin structure. Most of the current studies have focused on the methacrylation of lignin. The addition of epoxy functional groups for lignin macromolecules is an emerging study area in the coating industry, and the extension of this for SLA and DLP printing techniques can be insightful.[131] Additionally, further studies on fine-tuning lignin's UV absorption and radical scavenging properties will be beneficial for adding lignin at higher loadings in SLA and DLP techniques.

3.3. Direct ink writing (DIW)

Direct ink writing (DIW) is an extrusion-based 3D printing technique in an ambient environment. The essential part is developing printable paste-like inks or slurries with shear-thinning behaviors, allowing for smooth flow upon certain pressure. DIW is relatively simple and suitable for various materials, enabling the fabrication of macroscopic 3D complex materials.[132] Regarding the lignin inks for DIW, there are two main groups based on lignin sources: commercially separated technical lignin (alkali lignin, kraft lignin, *etc.*) and lignocellulose biomass, where the biomass is not bleached/delignified and used as a whole source. The molecular structure and physicochemical properties of these lignins vary with the selected isolation technologies, leading to different printability (printing resolution, shape fidelity, and geometry complexity) and performance of final 3D-printed materials.[133]

3.3.1. Isolated technical lignin used for DIW. Isolated lignin extracted from lignocellulose biomass is adopted as a component of the inks for DIW, as it is commercially available and accessible. Water is the most common medium for lignin inks or slurry in DIW. The isolated lignin shows poor dispersibility in water medium, resulting in inhomogeneous and unstable slurries. Therefore, various rheological modifiers were selected to improve its stability in water and the corresponding printability. For example, water-soluble alkali lignin (kraft lignin) and graphene oxide were mixed to get a homogeneous aqueous solution, 3D-printed by DIW and subsequently pyrolyzed into graphitic materials.[134] In this work, lignin was used as the carbon precursor, and graphene oxide acted as the viscosity modifier, resulting in homogeneous and printable inks. In another work, a water-based colloidal bio-ink comprising cellulose nanofibers and submicron black carbon derived from spherical lignin particles was developed as a sustainable alternative to traditional black fossil-based pigments.[135] Here, cellulose nanofiber was used as a binder and rheology modifier, where the particle-nanofiber network and particulate nature contributed to the multiple internal reflections and light-trapping, resulting in its super blackness. A soft triblock copolymer (Pluronic F127) was incorporated into the water dispersion of lignin, acting as the crosslinking agent to improve the rheological properties and water retention of the lignin-based ink, as shown in Fig. 6A–D.[66] The obtained lignin ink showed stiff and self-supporting features, preventing structural collapse during the DIW (Fig. 6E–G).[66] Compared to 3D-printed cellulose, the printed lignin-based objects showed superior water stability because of their intrinsic hydrophobicity, whereas the 3D-printed objects can maintain their integrity in water even under stirring. Gleuwitz *et al.* showed a flow-induced supramolecular arrangement created by DIW or shear casting the blend solutions of hydroxypropyl cellulose and organosolv

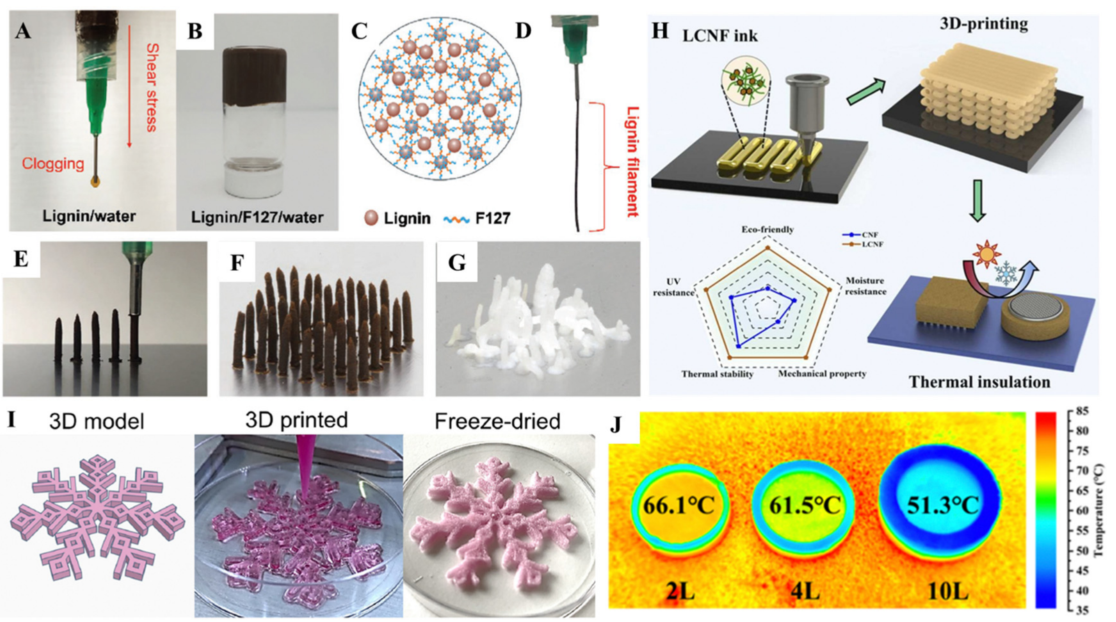

Fig. 6 Direct ink writing (DIW) of lignin materials. A digital image of (A) the lignin/water ink and (B) the lignin/F127/water ink (with 50 wt% of lignin) stored in an inverted vial to demonstrate its high viscosity. (C) Schematic of the interaction of lignin with F127. (D) Digital image of a lignin/F127/water filament extruded from a syringe with improved lignin printability. (E) and (F) Images of the vertical printing of lignin and (G) cellulose (cellulose cannot form a free-standing structure *via* vertical printing).[66] Copyright 2020, Wiley-VCH. (H) Schematic illustration of the manufacturing strategy for 3D printing of the customized LCNF aerogel for thermal insulation of electronics and a radar chart comparing the various physicochemical properties of 3D-printed CNF and LCNF aerogels.[68] Copyright 2023, Elsevier. (I) 3D model, wet 3D-printed snowflakes before crosslinking (wet conditions) and after crosslinking (freeze-dried).[137] Copyright 2021, Elsevier. (J) IR images of the printed battery insulated cap with different specifications on a hot stage.[68] Copyright 2023, Elsevier.

lignin and then locked *via* esterification with bio-based polycarboxylic acids.[136] The flow-oriented microstructure of shear cast films led to optical and mechanical anisotropy. This work highlighted the utilization of lignin as an essential additive for forming highly anisotropic cellulose-based materials.

Lignin is a binding agent in natural wood, providing wood strength, water stability, and cell wall rigidity. This enhances the mechanical properties and stability of various materials. The utilization of DIW stands out as a favorable method for configuring 2D planar nanomaterials like g-C_3N_4 semiconductors and MXenes, leading to a significant enhancement in their performance. However, the practical use of these 3D-printed materials in liquid reactions is restricted due to the weak interaction among the 2D planar structures. Inspired by wood structures, Jiang *et al.* used lignin as a binder and a vertical DIW strategy to build vertically aligned and hierarchically porous g-C_3N_4/CNT arrays.[138] The vertically aligned and hierarchically porous structure enhanced light harvesting capability and abundant surface active sites, resulting in outstanding photoelectrochemical hydrogen evolution performance. Thakur *et al.* replicated the natural wood compositions by creating water-based viscoelastic 3D printable inks with lignin, cellulose nanofibers (CNF), and cellulose nanocrystals (CNC).[67] By carefully tuning the ratios of each component and investigating their corresponding rheological behaviors, high-resolution printability was achieved, and the optimal formulation of components was very similar to that of natural wood. The 3D-printed objects *via* DIW were freeze-dried and then densified and consolidated by hot pressing.

Except for the use of technical lignin powder, lignin can be engineered into nanobeads/nanoparticles prior to the adoption of DIW inks. Spherical colloidal lignin nanoparticles were used to tune the properties of cellulose nanofibrils and alginate composite hydrogels for DIW, where adding 25% lignin nanoparticles improved printing resolution.[139] Moreover, lignin nanoparticles provided beneficial antioxidant properties to the final composite hydrogels and showed no negative effect on cell proliferation in the final printed scaffolds. Notably, lignin nanoparticles provide additional cross-linking sites for metal ions, leading to a high swelling ratio.

3.3.2. Lignocellulose biomass used for DIW. In general, lignocellulose biomass needs to be mechanically and/or physically pre-treated before being incorporated into the inks for DIW. Starting from unbleached poplar pulp, two different kinds of inks (with or without bleaching) were developed for DIW and subsequently lyophilized by freeze-drying, resulting in 3D-printed lignocellulose aerogels.[68] In this work, compared to pure cellulose nanofibril aerogels, the existence of lignin endows the final 3D-printed lignocellulose nanofibril aerogels with good UV and moisture resistance, as well as enhanced mechanical properties (Fig. 6H). The obtained 3D-printed porous biomass aerogels possess low density and low thermal conductivity, implying significant potential as customized thermal insulation materials (Fig. 6J). Baniasadi *et al.* presented the direct-ink writing of bio-hydrogels, consisting of aloe vera and cellulose nanofibrils (Fig. 6I).[137] The cellulose nanofibril-reinforced aloe vera bio-hydrogels displayed excellent rheological properties, allowing for smooth extrusion of thin filaments through a nozzle with a diameter of 630 μm. The wet stability and mechanical properties of 3D-printed composite hydrogels and subsequently freeze-dried aerogels improved with the enhancement of cellulose nanofibrils, attributed to the high aspect ratio of the nano- and microfibrils and their uniform dispersion in the aloe vera.

Lignocellulose biomass sourced from sugarcane bagasse was pulverized, sieved, and then dispersed in water at a high concentration of roughly 50 wt%, forming a smooth paste for DIW without additional additives.[140] This work used a relatively large nozzle size of 1.28 mm diameter, reflecting its unsatisfactory 3D printing resolution. Customized food package casings were 3D-printed, presenting good biodegradability and having potential as an alternative to petroleum-based plastics in the food packaging field. Gokce Bahcegul *et al.* demonstrated the 3D printability of alkaline extract corn cobs containing hemicellulose and lignin, where lignocellulosic biomass was adopted in its crude form, and no additives were involved.[141] Corn cobs were subjected to alkaline extraction by a 5% KOH solution and filtered to remove the insoluble part. The remaining solution was concentrated and became a gel at room temperature. It was printed by DIW and post-immersed in ethanol to fix the printed geometries.

Inspired by the natural wood warping phenomenon caused by an uneven volumetric change due to fiber orientation, Kam *et al.* showed that by predesigning the 3D printing pattern and flow rate, they could dictate the alignment and intensity of the 3D-printed objects, resulting in programmed warped geometry after drying.[69] The ink developed in this work consists of industrial polydisperse wood powder and plant-extracted natural binders: CNC and xyloglucan. The shape-programming capability was demonstrated by printing elongated ribbons composed of two perpendicular layers of cylinders, in which the printing direction matched the axes of the ribbon and helices and was rotated by $\pm 45^\circ$ with respect to these axes.

In summary, additives are indispensable for 3D-printed lignin materials *via* DIW, whether for isolated lignin or lignocellulose biomass, because of the poor interaction between lignin or whole lignocellulose biomass and water. The primary function of these additives is to optimize the stability and homogeneity of the inks. Keeping sustainability in mind during the material selection, bio-source additives are prioritized, and the amounts of additives adopted should be limited or eliminated.

Deep eutectic solvent (DES) is a green solvent system with a higher evaporation pressure than water or other organic solvents used for DIW, which endows DES-based slurries with enhanced stability and a broader process window during DIW. DES pretreatment combined with mechanical processes could break down the recalcitrant lignocellulose structure, resulting in finer lignocellulose slurries, preventing clogging during printing, and allowing for smooth and high-resolution DIW. There are some reports on using cellulose nanocrystals (CNC) and cellulose nanofibers (CNF) in DES for DIW, from which conductive and flexible eutectogels were obtained for sensors.[142,143] So far, there has been no related work on using lignocellulose biomass in DES for DIW.

3.4. Selective laser sintering (SLS)

Selective laser sintering (SLS) is a 3D printing process based on a layer-by-layer fusion of powders using a CO_2 laser source, where the heated powders sinter to form a solid layer. Thus, powders such as metals, ceramics, and some polymers, which could be fused under a laser beam and solidified when the temperature decreases, are ideal for SLS.[70] The raw powders for SLS are generally composed of a high-melting-point powder and a low-melting-point powder. Regarding the adoption of lignin in SLS, there are two forms: commercial lignin powder and wood flour containing lignin. For example, alkali lignin was compounded with polyamide at a concentration of up to 60 vol% for SLS to realize complex structures. Adding lignin improves the stability of the raw materials during sintering, with 30% less degradation compared to the neat polyamide.[70] In 2004, wood powder–plastic composites were proposed for the first time as sustainable and low-price feedstock of SLS.[144] Wood flour and a hot-melt adhesive powder (polyester) were mixed for SLS. The polyester melts bind to the wood powder under laser radiation and then solidify to form a consolidated complex object.[145] In summary, SLS is not as popular as the other three techniques for 3D printing of lignin materials, and only a few works have been reported.

4. Lignin-based smart materials and 4D printing of lignin materials

4.1. Lignin-based smart materials

In recent years, there has been a significant focus on enhancing lignin for developing new sustainable materials, leveraging its attractive properties such as thermal stability, high carbon content, biodegradability, antioxidant, UV absorbance, and antimicrobial activity.[146] Thus, the emergence of lignin-based smart materials capable of responding to external stimuli like pH, temperature, light, or electricity represents a new frontier in value-added applications. The smartness of lignin materials is mainly realized through the chemical modification of lignin for conjugated lignin–polymer systems and the copolymerization of lignin with other polymers, using the chemical modification and polymerization methods summarized in Section 2. Integrated with 3D printing, lignin-based smart materials demonstrated their potential for 4D printing scenarios.

4.1.1. Lignin-based shape memory polymers. Shape memory polymers (SMP), a class of stimuli-responsive materials, possess the ability to revert to their original state after adopting a temporary shape induced by exposure to light, heat, or magnetic/electrical stimulation.[147] Jin *et al.* utilized lignin's rigid benzene ring structure and outstanding photothermal properties due to lignin's conjugated system to create light-driven lignin-based shape memory polymers (ELEP).[148] This work used enzymatically hydrolyzed lignin (EL), epoxy soybean oil (ESO), and polyethylene glycol (PEG 400) to form robust 3D networks. Increasing the EL proportion from 40 to 60 wt% significantly improved mechanical properties, including increased tensile strength and T_g. Under simulated solar irradiation, ELEP50 (50 wt% lignin) exhibited rapid shape memory behavior across multiple cycles. The same group also worked on developing recyclable lignin-based light-driven shape memory polymers by combining lignin's rigid structure with dynamic ester bonds.[149] Enzymatic lignin epoxy resin with dithiodibutyric acid exhibited excellent mechanical properties, high shape fixation and recovery rates, and notable photothermal effects. These works showcase the potential applications of lignin-based light-driven shape memory polymers with recyclability. In addition, Liu *et al.* investigated the incorporation of four types of lignin into polyester polyols to synthesize lignin-based polyurethane foams (PUFs).[150] The lignin's functional groups, notably –COOH and aliphatic –OH, positively correlated with polyol miscibility, influencing the resulting cellular structures, density, and compressive modulus of PUFs. The thermo-responsive shape-memory properties of these PUFs demonstrated increased T_g and promising stretch fixity and recovery ratios. In summary, the light absorption of lignin in SMP is influenced by its concentration, which could enhance the photothermal efficiency and other properties of SMP. Identifying optimal concentrations and effective UV-visible wavelengths of lignin can facilitate the performance optimization of SMP.

4.1.2. Lignin-based self-healing polymers. Self-healing polymers can recover from physical damage through various approaches, including diffusion, flow, shape-memory effects, and covalent-bond reformation,[151] transforming a polymer into a "smart material". Sun *et al.* explored a novel approach to creating lignin-containing PU elastomers from corn stover inspired by biological self-healing mechanisms.[152] They employed a strategy involving hydrogen and disulfide bonds, achieving elastomers with tensile strength (10.77 MPa) and self-healing properties (>93%), where the aromatic ring structure of lignin contributes to enhanced tensile strength, while the synergy of dynamic hydrogen and disulfide bonds improves self-healing capabilities (Fig. 7A). This work introduces a high-value application of lignin for developing sustainable smart materials. On the biomedical front, a novel polymer system was developed by Han *et al.*; their work incorporated sulfonated lignin, creating a supramolecular hydrogel dressing with enhanced mechanical strength, self-healing, antioxidant activity, and biological performance.[153] Their study showed that sulfonated lignin boosts stress values by over tenfold and achieves a good 95.53% self-healing efficiency. *In vitro* tests confirm nontoxicity and good biocompatibility using a rat wound healing model. The hydrogel dressing shows potential for wound management by maintaining a moist environment, promoting healing and reducing inflammation. This lignin-based hydrogel presents a promising solution for effective wound treatment.

On a related note, vitrimers are a relatively new class of materials marked by dynamic covalent bonds in crosslinked

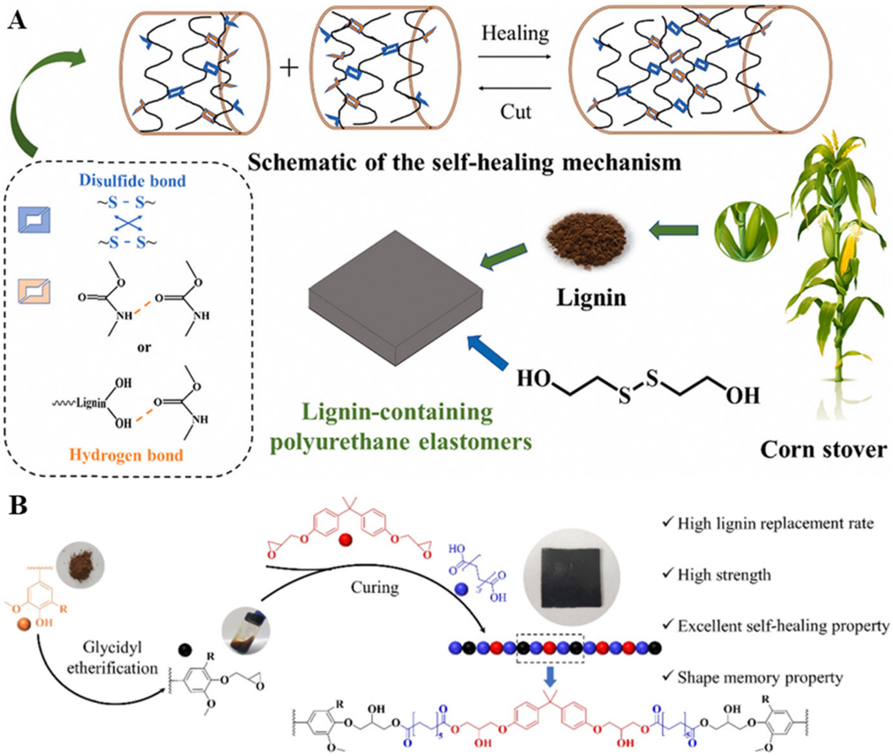

Fig. 7 (A) Schematic overview of lignin-based PU with self-healing properties.[152] Copyright 2021, Elsevier. (B) Schematic overview of the development of a lignin-based vitrimer as a sustainable alternative to bisphenol A epoxy resin.[154] Copyright 2021, Elsevier.

networks. These networks undergo thermally stimulated exchange reactions, enabling them to be processed like vitreous glass without losing integrity.[155] Lignin-based vitrimers, derived from lignin's abundant hydroxyl groups, have been explored in various studies.[154] A study done by Xue *et al.* focused on developing lignin-based epoxy vitrimers with high mechanical strength and lignin replacement rates by gradually substituting diglycidyl ether bisphenol A with glycidyl ether of lignin (Fig. 7B).[154] Remarkably, at a 100% lignin replacement rate, the vitrimers demonstrated a tensile strength of 39.5 MPa and an elongation at break of 5.81%. Notably, these lignin-based epoxy vitrimers exhibited outstanding self-healing, reprocessing, and shape memory properties, with crack widths repaired over 80% in just 5 min at 160 °C and a 97% healing efficiency for tensile strength after hot reprocessing.

4.2. 4D printing of lignin materials

4D printing is a new type of 3D printing technique, endowing the transformation capacities of 3D-printed objects upon exposure to external stimuli, leading to changes in their shapes, properties, and functions.[156,157] Smart lignin materials show potential for 4D printing. The specific chemical modification of lignin materials enables 3D-printed objects to be responsive to external stimuli, such as heat, light, and humidity. Through 4D printing, a predictable and predefined time-dependent change in the functionality of 3D printable products could be achieved.[158] Therefore, integrating additive manufacturing and stimuli-responsive materials facilitates the flexible and precise construction of smart products.[159]

Lignin with conjugated structures was directly added into PLA *via* a melt blending process, where the modified lignin acted as the photothermal conversion module. The obtained lignin-containing filaments showed good 3D printing performance (FDM technique) and near-infrared light responsiveness (Fig. 8A).[71] Fig. 8C demonstrates that different 3D-printed structures showed excellent shape recovery behaviors. In another similar work, FDM was used to 3D print light-responsive shape memory composites made from PCL/TPU/lignin, in which lignin was used as a functional nanofiller due to its excellent photothermal conversion efficiency.[160] Moreover, lignin was proven to improve the rheological properties of the PCL/TPU composite and make it more suitable for FDM. A bioconjugate of keratin and lignin was developed in both water and solid states. The water state conjugates were processed in paste form for DIW, and the solid state ones were extruded into FDM filaments at temperatures >130 °C but accompanied by degradation.[72] These 3D-printed water-state bio-composites show mechanical responses to moisture stimuli upon water soaking. Wang *et al.* first used a controllable molecular assembling method *via* dialysis to make lignin nanotubes. Then, they incorporated them into polyurethane matrices for DIW, realizing ultraviolet light-responsive shape memory polyurethane composites, where lignin nanotubes acted as UV absorbents (Fig. 8B).[161] With the increased UV irradiation time, the shape of 3D-printed petals changed from a closed to an open state,

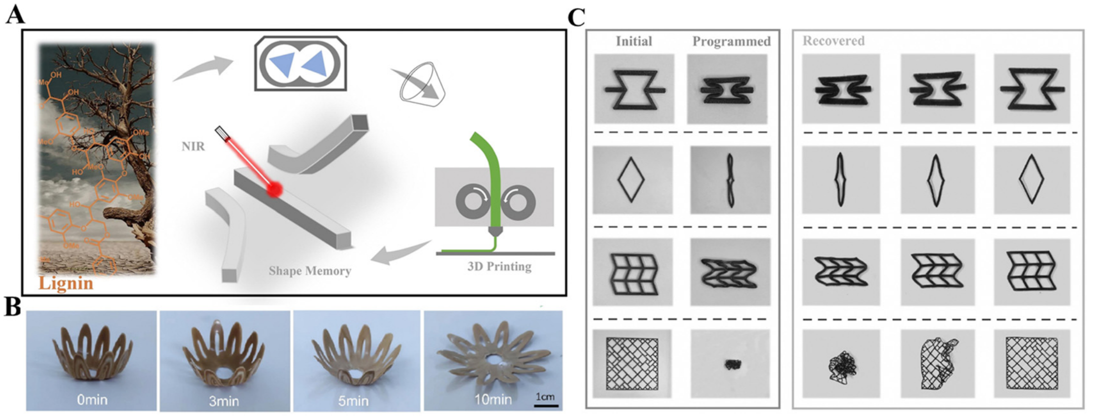

Fig. 8 4D printing of lignin materials. (A) Lignin as a photothermal module for shape memory composites.[71] Copyright 2023, Elsevier. (B) The shape recovery process of 3D-printed petals at different UV irradiation times (0–10 min). Under UV light, the petals change from buds to flowers.[161] Copyright 2023, Elsevier. (C) Shape memory for 3D printing different structures in a water bath at 70 °C.[71] Copyright 2023, Elsevier.

mimicking the process of development of actual flowers from bud to bloom. Ren *et al.* developed a composite filament for FDM, where lignin-coated Fe_3O_4 magnetic nanoparticles were prepared by combining co-precipitation and chelation methods and then incorporated into the poly(propylene carbonate)polyurethane/PLA composites.[159] Magnetic nanoparticles endowed the composites with shape memory behavior triggered by thermal and alternating magnetic fields and near-infrared radiation. In this work, adding lignin promotes the uniform dispersion of coated nanoparticles in the polymer matrix.

In previous reports on the 4D printing of lignin materials, lignin was incorporated into the shape memory or stimuli-responsive matrix to realize the smart materials or chemical modification was applied to endow lignin with stimuli responsiveness. Apparently, in the second case, the full use of lignin was made, and lignin is indispensable for the engineering of the final 4D-printed smart materials. In contrast, in the first case, lignin is just used as a filler for the smart matrix and could be easily replaced by other fillers. Also, lignin is not the main contributing component to the smartness.

5. Applications of 3D/4D-printed lignin materials

5.1. Biomedical applications

Bioactive materials are crucial in healthcare applications, including wound dressing and tissue engineering. Lignin exhibits a more excellent thermal stability than cellulose and hemicellulose and possesses hydrophobic properties (excluding lignosulfonates). Due to its antioxidant, antibacterial, anti-UV, antitumor, and antivirus properties, lignin stands out as a promising bioactive material.[32,162] Thus, incorporating lignin into printing inks can enhance their overall performance.[163] However, compared to other biopolymers, limited research has been conducted on 3D printing with lignin as the primary ink component. A recent review written by Graichen *et al.* highlighted the potential promise of scalable lignin-based products achieved through 3D printing.[164] Lignin materials are particularly promising for 3D printing, as some possess qualities that align with 3D printing and medical requirements. These include suitable printability, mechanical properties, biodegradability, biocompatibility, tissue biomimicry, and non-cytotoxicity.[165,166] Recently, there has been a significant focus on exploring various forms of lignin for biomedical applications, specifically as a carrier for drug delivery, attributed to its notable antioxidant properties.

In an investigation of lignin/PLA nanofibers, there was a progressive increase in antioxidant activity with higher lignin content. However, higher concentrations of lignin were observed to hinder cell proliferation.[167] Therefore, maintaining a balanced lignin concentration is crucial for achieving good biocompatibility. For FDM printing, filament formulations containing blends with thermoplastics are deemed suitable. In the case of DIW, ink formulations have advanced to incorporate water-based hydrogels, including hyaluronan, alginate, gelatin, and, more recently, cellulose nanomaterials.[168,169] Maintaining an equilibrium between the hydrophilicity and hydrophobicity of the matrix surface is essential for facilitating cell adhesion.[170] Consequently, including lignin, known for its hydrophobic nature, in hydrogels can be a strategy to adjust the hydrophilicity of the resulting matrix.[171,172] Dominguez-Robles *et al.* successfully extruded pellets consisting of PLA blended with castor oil, kraft lignin, and an antibiotic (tetracycline) using fused filament fabrication (FFF). This formulation enables the production of composites suitable for FDM technology, specifically designed for 3D printing applications in wound dressing.[173] It was found that minimal amounts of lignin in the composites lacked antimicrobial efficacy against *S. aureus*. Notably, the antimicrobial properties of the composites were primarily attributed to tetracycline. In this study, curcumin, used as a representative drug, was applied to the meshes to examine diffusion characteristics. The drug was observed to permeate through the mesh pores, reaching the wound easily. Interestingly, the introduction of lignin led to a slower release of curcumin compared to the control, and when combined with PVA, it further extended the release of curcumin. Possessing antioxidant properties, lignin plays a role in diminishing the concentration of reactive oxygen species closely associated with the pathogenesis of chronic wounds. This renders lignin/PLA a sustainable and cost-effective 3D printable biomaterial with an effective impact on wound treatment.

Another evolving application area involves the production of lignin-based nanoparticles as carriers for drug delivery.[174] The stability of such lignin-based nano-systems holds the potential for providing effective nano-delivery solutions in medical applications, particularly as hydrogel inks progress in the field of printing. With the progress in 3D printing technologies, the DIW 3D printing technique allows the printing of soft materials, including hydrogels. Oveissi *et al.* incorporated a physical crosslinker, lignin, into hydrophilic polyether-based polyurethane (HPU). The resulting hydrogel was fabricated through 3D printing using DIW and demonstrated biocompatibility with human dermal fibroblasts.[175] Their study revealed that adding 2.5 wt% lignin increased fracture energy, Young's modulus, and lap shear adhesiveness in the hydrogels. These improvements were attributed to enhanced hydrogen bonding within the hydrogel network. To assess biocompatibility, human dermal fibroblasts were cultured on the lignin-HPU film for up to 72 h. The outcomes indicated no significant changes in cell viability, indicating its ability to support cell growth and showing great potential in the biomedicine field.

Zhang *et al.* developed a bioink using a hydrogel DIW approach consisting of cellulose nanofibrils (CNF), alginate, and colloidal lignin particles (CLP).[176] Incorporating CLP into the CNF-alginate-CLP nanocomposite scaffolds introduced antioxidant properties, with the antioxidant behavior being dependent on CLP concentration added. Moreover, increasing CLP concentration increased hydrogel viscosity, enhancing the shape and 3D printing resolution. The scaffold maintained its structural integrity and viability when stored in Dulbecco's phosphate buffer for a period of 7 days. The scaffold also demonstrated a high water-retention capability, with the rehydration ratio exceeding 80%. Notably, no adverse effects on the HepG2 hepatocellular carcinoma cell line were observed when CLPs were added. The HepG2 cells exhibited proliferation both internally and externally on the porous scaffolds, suggesting excellent biocompatibility.

The controlled-release properties of lignin composites can be tailored using SLA or DLP techniques. The DLP 3D printing method depends on the photopolymerization of a photopolymer matrix with the inclusion of photoinitiators. To address this, a one-step esterification reaction was conducted to synthesize two alkylated derivatives of dealkaline lignin, namely DAL-11ene and DAL-12ane. This reaction involved the interaction of dealkaline lignin (DAL) with undecanoyl chloride and dodecanoyl chloride.[33] DAL-11ene and DAL-12ane displayed superior photo-initiating capabilities in comparison to DAL. As an additional photoinitiator for DLP 3D printing, ethyl 4-(dimethylamino)benzoate (EDAB) was incorporated as a co-initiator. The release of the two polymeric tablets initiated by DAL-11ene/EDAB and DAL-12ane/EDAB in methanol decreased compared to that of Irgacure2959. The biosafety of these produced polymeric tablets was further assessed through live/dead staining. The results showed strong proliferation and growth of L929 cells on the tablet surface, with cell density significantly surpassing that of the control group. Increasing the concentration of either DAL-11ene or DAL-12ane showed no apparent difference, highlighting the polymeric tablets' exceptional biosafety and cytocompatibility. Therefore, the effectiveness of DLP 3D printing was effectively demonstrated by integrating a photoinitiator into the 1,6-hexanediol diacrylate (HDDA) monomer, indicating the potential of the printed composites for applications in packaging and environmentally friendly photopolymerization materials.

A research team explored the synergistic combination of curcumin, lignin, and poly(caprolactone) (PCL) to develop wound dressings with antioxidant and antimicrobial properties.[177] D-Panthenol was also included for its skin regenerative abilities by improving epidermal differentiation. Using semi-solid extrusion (SSE) 3D printing without solvents (Fig. 9A), the dressings provide sustained release of D-Panthenol and curcumin for up to 4 and 35 days, respectively. They exhibit higher resistance to *Staphylococcus aureus* adherence, with reduction of up to 98.9% compared to PCL control 3D printing samples. *In vivo* studies on Wistar rats demonstrate marked improvement at all stages of treatment, and histological examination reveals superior outcomes in terms of epithelization, inflammatory reaction, fibroblast proliferation rate, and neoangiogenesis for wound dressings. Cytocompatibility and the structures printed in 3D are illustrated in Fig. 9B. Fig. 9C shows that the epidermis regeneration was complete in all samples after 13 days of treatment.

5.2. Environmental and energy applications

Recently, there has been growing interest in exploring lignin for its potential use in manufacturing electronics such as batteries and supercapacitors, catalysis, and environmental remediation, serving as a pollutant adsorber and precursor. A key benefit lies in its eco-friendly nature, and the growing production of lignin in the past few decades has made it more accessible at a lower cost. Due to its redox functionalities, lignin plays a crucial role in diverse energy conservation processes involving reversible oxidation/reduction reactions like those found in respiration and photosynthesis. The significant carbon content exceeding 60 wt% makes lignin highly valued for producing energy materials. The presence of benzyl and phenolic groups in lignin serves as active reaction sites for the storage of ions in applications like supercapacitors. Additionally, the high number of oxygen atoms present in lignin also aids in facilitating electrolyte ion adsorption and redox reactions. The favorable cross-linked structure of lignin makes it a suitable choice for developing porous carbon structures in supercapacitors.[178]

Lignosulfonates, preferred for their ability to function as sulfur-doped agents in batteries or supercapacitors, are favored for such applications. Meanwhile, alkali lignin has demonstrated suitability for electrospinning to produce

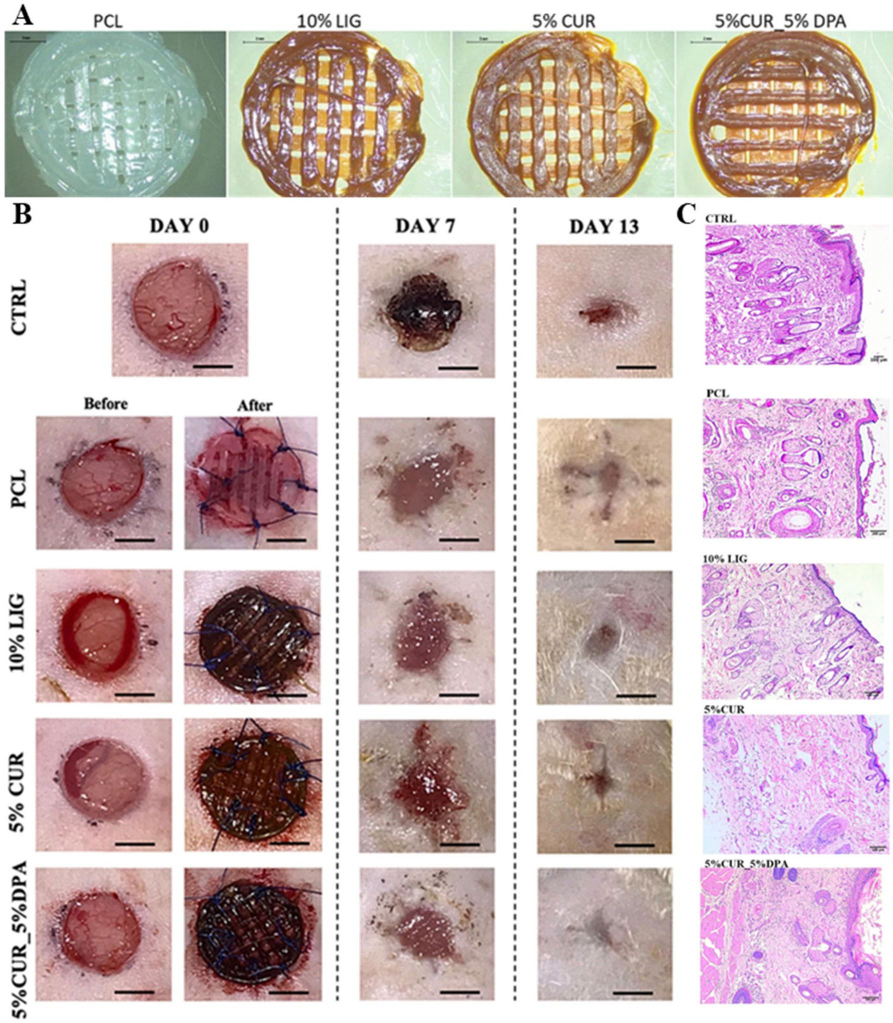

Fig. 9 3D-printed lignin materials for biomedical applications. (A) Microscopic images captured under a light microscope showcase 3D-printed wound dressings comprising varying weight proportions of PCL, lignin, curcumin, and DPA. The scale bar is 2 mm. (B) Evaluation of wound healing in Wistar rats involved a macroscopic assessment of progression days 0, 7, and 13. The analysis encompassed untreated (CTRL) and treated rats with 3D-printed dressings sutured over the wound, both before and after applying the examined dressings (scale bar: 5 mm). (C) Wound healing microscopic analysis with semi-quantitative assessment on day 13 after surgery for each condition and CTRL. Representative histological haematoxylin & eosin (H&E)-stained images of the wound sites.[177] Copyright 2023, Elsevier.

nanomaterials.[179] In energy material applications, carbon can typically be obtained from lignin through two commonly used processes. One method involves precursor carbonization followed by carbon activation, whereas the other method employs chemical activators concurrently with carbonization and activation.[178] Graphene, a promising carbon material for electrochemical energy applications, can be synthesized from lignin through processes such as catalytic graphitization, carbonization, or oxidative cleavage coupled with aromatic refusion.[180,181]

Graphitic structures with adjustable density were showcased, achieved through DIW of lignin/GO inks, followed by subsequent carbonization (Fig. 10A and B).[182] By altering the lignin proportion, it is feasible to customize the density and graphitic order to meet specific requirements, resulting in distinct electrical and mechanical properties. Adjusting the ratio of lignin allows the possibility of customizing the density and graphitic order to fulfill specific requirements, resulting in distinct electrical and mechanical properties. It was found that the conductivity of graphene oxide was initially low at 14 S cm^{-1}, but a significant increase was observed in lignin/GO with a 70/30 composition, reaching 560.5 S cm^{-1} (Fig. 10C). The overall density and pore volume of the produced structure can be precisely adjusted over a wide range, spanning from 0.2 to 1.8 g cm^{-1} and 0.024 to 0.12 cm^3 g^{-1}, respectively (Fig. 10D). The adjustable electrical and mechanical characteristics of carbon materials derived from lignin render them highly promising for various applications, including supercapacitors and batteries.

A research group has also demonstrated a simple method, employing femtosecond laser direct writing, to convert lignin into porous conductive carbon structures and interdigitated

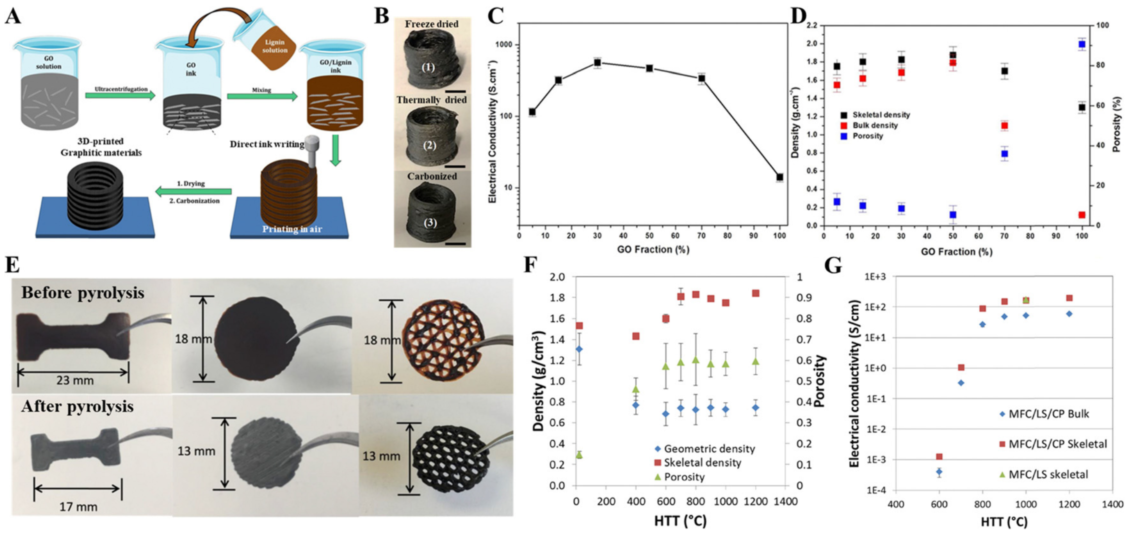

Fig. 10 3D-printed lignin-based carbon composites for electronic applications. (A) Illustration of the fabrication process of DIW-printed lignin/GO-based carbon materials, (B) photos of 3D-printed objects in different processes (freeze-dried, thermally dried, and carbonized), scale-bar is 5 mm, (C) changes in electrical conductivity, and (D) variations in density and porosity of lignin/GO-based carbon materials over time.[182] Copyright 2020, Elsevier. Photos of 3D-printed objects from MFC/LC/CP hydrogels after (E) air-drying and pyrolysis at 1000 °C, (F) changes in density and porosity of MFC/LS/CP carbons as a function of heat-treated temperature, (G) elastic modulus of MFC/LS/CP monolines pyrolyzed at different HTTs from 3-point bending tests.[183] Copyright 2018, Elsevier.

circuits to advance supercapacitor devices.[184] It was found that the supercapacitor utilizing lignin/PAN demonstrates high elevated areal specific capacitance, reaching 6.7 mF cm^{-2} (0.9 F cm^{-3}) at a scan rate of 10 mV s^{-1}. However, adding mixing functional materials (MoS_2) to the materials demonstrated higher areal capacitances, reaching up to 16 mF cm^{-2} (2.2 F cm^{-3}) at 10 mV s^{-1}. This shows that the suggested method could produce energy storage devices using natural lignin. Shao *et al.* conducted a study employing blends of microfibrillated cellulose (MFC), lignosulfonate (LS), and cellulose powder (CP) to produce conductive and durable carbon structures through 3D printing followed by pyrolysis.[183] The 3D-printed MFC/LS/CP material demonstrated high printing precision, self-standing capability, and stability after air drying and pyrolysis (Fig. 10E–G). It was found that at a temperature of 900 °C, MFC/LS/CP carbons not only exhibit a notable electrical conductivity of 47.8 S cm^{-1} (Fig. 10G) along with a low bulk density of 0.74 g cm^{-3} (Fig. 10F) but also attain an elastic modulus of 6.6 GPa. The adjustable electrical and mechanical characteristics of carbon materials derived from lignin render them highly promising for various applications, including supercapacitors and batteries.

Lignin, characterized by its aromatic nature and carbon content, possesses the potential to create graphene-like structures applicable in energy-related contexts. Faisal *et al.* illustrated the production of porous graphene through direct laser writing, utilizing photothermal induction from Kraft lignin.[185] The resulting laser-induced graphene (LIG) exhibited a hierarchical structure featuring a 3D interconnected network that facilitated its transfer from the kraft lignin/poly(ethylene oxide) (KL/PEO) film onto polydimethylsiloxane (PDMS). The supercapacitors constructed with LIG/PDMS composites showed promising electrochemical performance and exceptional cyclic stability, retaining over 90% capacitance after 10 000 cycles, which could have significant potential for developing portable and wearable electronics. In a study conducted by Ye *et al.*, a straightforward method was introduced to employ CO_2 laser scribing to transform wood surfaces into hierarchically porous graphene.[186] The patterns observed on wood surfaces predominantly originate from lignin, enabling the material to function as an electrode for energy generation or as a supercapacitor for energy storage. Zhang *et al.* have provided additional evidence that lignin films can undergo a direct conversion into graphene electrodes through CO_2 laser exposure, showcasing commendable electrochemical capabilities.[187] Studies have also shown that lignin is a valuable component in nanofluidic composite membranes, enhancing both efficient ion transport and the harvesting of osmotic energy.[188] Specifically, it was discovered that lignin not only aids in the effective dispersion within the sulfonated PEEK matrix but also greatly enhances the proton conductivity and ion selectivity. This improvement positions the membrane as a promising device for advancing larger-scale vanadium redox flow batteries in the next generation.[189] In essence, the advancement of lignin 3D printing and functional materials represents a pivotal step towards advancing advanced materials.

By integrating the adhesive properties of lignin with 2D planar nanomaterials, the 3D-printed structural composites can significantly broaden lignin potential applications, particularly in stable structures. Jiang *et al.* have reported enhanced photoelectrochemical hydrogen evolution performance by vertically 3D printing arrays resembling a forest comprising lignin/g-C_3N_4/carbon nanotubes (CNT) (Fig. 11A and B).[190] The incident light path is extended by the multiple scattering occurring within the arrays. Simultaneously, the CNT plays a role in further enhancing the effective separation of photoelectron-hole pairs, thereby improving light utilization and photoelectron transfer efficiency (Fig. 11C). The 3D-printed arrays exhibit high durability due to the inherent hydrophobicity and strong adhesivity of lignin, allowing for continuous hydrogen production. Additionally, the aromatic nature of lignin, coupled with intermolecular π–π interaction between lignin and g-C_3N_4, is believed to create a donor–acceptor conjugated structure. This intermolecular π–π interaction results in an improved photoelectrochemical hydrogen evolution performance. It was also illustrated that lignin, serving as a natural binder, surpasses other binders like PVA and PEG in terms of adhesivity. This superiority may arise from the non-conductive and long-chain molecular structures of PVA and PEG, which hinder the generation and separation of photoelectrons. Given the global

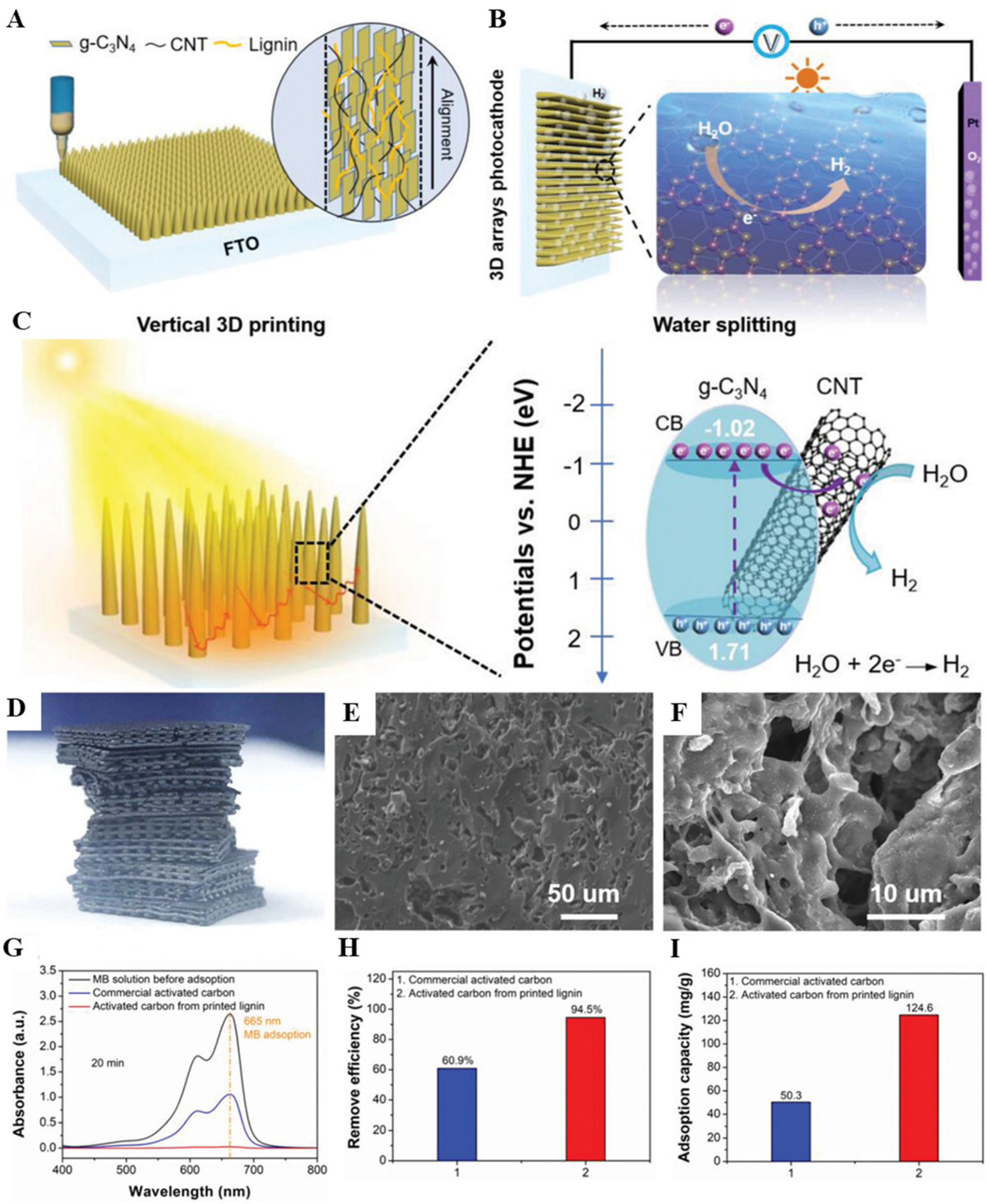

Fig. 11 Structural composites designed for photoelectrochemical hydrogen evolution. (A) Vertical 3D printing of g-C_3N_4/CNT/lignin on a conductive substrate and its microstructure, (B) schematic representation of the photoelectrochemical water splitting process using the printed arrays as the photocathode, and (C) photoelectrochemical mechanism for the printed arrays.[190] Copyright 2019, Wiley-VCH. Activated carbon derived from 3D-printed lignin-based scaffolds for water treatment. (D) Photo of activated carbon obtained from the 3D-printed lignin scaffold, (E) and (F) surface morphology of activated carbon originating from the 3D-printed lignin scaffolds, (G) UV-vis spectra of methylene blue (MB) solutions after 20 min of adsorption by the activated carbon from printed lignin and commercial activated carbon (the characteristic adsorption peak of MB is situated at 665 nm), and the comparison of (H) removal efficiency during static adsorption after 20 min for the active materials and (I) adsorption capacity of commercial activated carbon and activated carbon derived from printed lignin.[191] Copyright 2020, Wiley-VCH.

overconsumption of fossil fuels, materials incorporating green and renewable biomass as components present a new opportunity for the sustainable production of clean energy.

Through the integration of 3D printing, the active carbon materials produced from printed lignin have shown significantly enhanced adsorption efficiency compared to commercial carbon materials.[191] Initially, as part of the carbonization and activation processes, the compact structure of the printed lignin filaments undergoes a conversion into a porous state, where the micro-level pores within these filaments play a vital role in enhancing the efficiency of mass transfer (Fig. 11D–F). Moreover, the spacing between neighboring filaments is modifiable, contributing to forming a hierarchical porous structure in the resulting product. The UV-vis spectra (Fig. 11G) indicate that the methylene blue (MB) adsorption peak nearly vanished in the activated carbon derived from the printed lignin scaffold. In contrast, MB persists in the solution for commercial activated carbon. It was also found that the activated carbon from printed lignin has a removal efficiency of 94.5%, significantly surpassing the lower efficiency observed for the commercial activated carbon (Fig. 11H). Furthermore, the adsorption capacity of the activated carbon derived from the lignin scaffold reaches 124.6 mg g^{-1}, marking a 2.48-fold increase compared to the commercial activated carbon (Fig. 11I). Additionally, the active carbon with 3D scaffolds facilitates multiple recycling, offering a practical and sought-after method for treating industrial pollutants.

5.3. Other applications

Moreover, 3D/4D printing has enabled other applications for lignin materials. Goretti *et al.* developed a flexible and portable pressure sensor using DLP, consisting of polyaniline, lignin, and acrylate.[192] Adding lignin into the filler polyaniline improved its dispersion and integration within the acrylic matrix, facilitating 3D printing and improving the performance of the printed objects. A piezocapacitive prototype transducer was built from the printed composites, which shows a response to a human footfall and transmit its corresponding electrical signal. Yu *et al.* reported the fabrication of a triboelectric nanogenerator (TENG), in which the insoluble and infusible biomass (lignin and chitosan) was employed in a polyamide matrix by FDM.[193] It is notable that the microstructure formed inside the friction layer, due to the extrusion of the printing and the different degrees of thermal expansion and contraction of biomass and the matrix, increasing the surface roughness and the actual contact area, thereby effectively improving the triboelectric properties of the lignin-based TENG. Shao *et al.* reported that lignin-based biocarbon with good electrical conductivity was prepared by 3D printing and subsequent pyrolysis.[183] The 3D-printed lignin-based biocarbon precursor showed excellent morphological stability, although a significant shrinkage occurred during the pyrolysis.

Besides the abovementioned applications, lignin could be used as a structuring material, providing mechanical reinforcement to the 3D-printed matrix, considering that naturally, lignin is the strengthening part of plant cell walls.[61,66] For example, adding softwood kraft lignin to methacrylate resin can enhance the mechanical properties of 3D-printed composites *via* SLA.[61]

6. Sustainability consideration and management

Advancements in technology and the growing emphasis on sustainability have inevitably led to the exploration of merging two popular fields: 3D printing and lignin-related research. Lignin holds significant potential for advancing sustainable manufacturing, particularly in reducing carbon emissions, conserving energy, and minimizing waste. Comprising approximately 60–65% carbon, lignin effectively sequesters carbon when integrated into materials, preventing its release into the atmosphere. Replacing fossil-based products with lignin-based alternatives can reduce emissions. For example, lignin-derived polyurethane foams can lower emissions by 30–50% compared to traditional petroleum-based foams. In terms of energy efficiency, incorporating lignin as a filler in epoxy resins shows a 40% energy reduction compared to conventional epoxy resins, attributed to the low energy consumption during raw material production.[194] Despite the global production of over 50 million tons of lignin annually as a byproduct of the paper and pulp industry, only about 2% is currently valorized.[32,195] Increasing lignin utilization presents a significant opportunity to reduce landfill waste and enhance resource sustainability.

It is frequently taken at face value that using green materials implies that the work is sustainable. Yet, such recognition is too simplistic, and it is often not the case. Therefore, this section will delve into the green approaches developed for the 3D printing of lignin materials. Specifically, the advances are examined in three different parts: (i) lignin extraction/modification, (ii) biodegradation/recyclability of 3D-printed lignin materials, and (iii) the efficient use of biomass *via* additive manufacturing.

6.1. Green chemistry and green solvents for lignin extraction/modification

As mentioned in the earlier section, lignin holds the potential to replace petroleum resources. It is, therefore, of great interest to investigate the different means to extract it. Given the heterogenous and intractable structure, it is necessary to modify lignin, especially to improve its solubility, before it can be used in applications. The challenge lies in making the extraction and modification processes green and sustainable. Much research effort has surrounded these goals. This is crucial as using green materials alone is insufficient to be considered sustainable unless the methods employed are also sustainable. At present, as shown in Fig. 12, multiple approaches have been developed, including use of green reagents such as alternative green solvents (*i.e.*, ionic liquids[196–198] and deep eutectic solvents,[199–201]) and green catalysts (*i.e.* enzymes[202,203]), using a solventless reaction,[204,205] streamlining to one-pot synthesis,[205–208] having

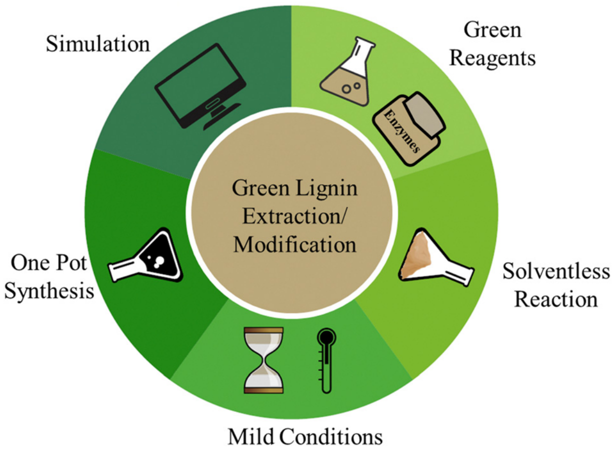

Fig. 12 Green strategies for lignin extraction/modification.

milder conditions,[197,209,210] and reducing energy inputs required. Other possible methods are to perform stoichiometric calculations of the required reagents instead of adding excessive reagents and to improve the yield per synthesis given the same inputs. Simulations could potentially be the way to achieve high yield with minimal reagent wastage. Mohan *et al.* have used molecular dynamics simulations to estimate the solubility parameters of lignin, ionic liquids, and deep eutectic solvents.[211] The best solvent to use for biomass delignification was identified. The technique was validated by the results obtained from both experiment and simulation.

6.2. Biodegradation/recyclability of 3D-printed lignin materials

Another important factor to consider for sustainability management is the biodegradability and recyclability of the 3D-printed lignin materials, as the materials should not accumulate in the waste pile, which can affect the ecology in the long run. Using renewable and biodegradable resources, such as lignin, to replace non-renewable materials is aligned with the sustainable aim. While lignin does not surpass cellulose and hemicellulose in terms of biodegradation within biomass, it remains biodegradable compared to petroleum-based materials.[212] The biodegradation behavior of lignin varies depending on its state. In its native form within lignocellulosic biomass, lignin is highly cross-linked and associated with cellulose and hemicellulose, retaining intact β-O-4 ether bonds. By contrast, isolated or extracted lignin is more readily degraded due to partial depolymerization, the cleavage of β-O-4 ether bonds, and increased surface exposure during the extraction process.[213] Consequently, native lignin within whole lignocellulose biomass degrades more slowly than extracted lignin. However, the presence of cellulose and hemicellulose in the lignocellulose biomass facilitates a higher overall biodegradation rate in 3D-printed biomass materials, which also depends on the biomass sources and the relative ratios of each component. Additionally, it is important to highlight that the biodegradability of lignin-based materials remains insufficiently understood, with only a few studies addressing this topic. This presents a promising avenue for further investigation in future research.

However, it is inadvisable to categorize lignin-based materials as sustainable just because lignin is present. Lignin has been extensively explored with various materials for 3D printing, ranging from thermoplastic PU[214] and PLA[96] to vanillin and soybean oil.[126] Two strategies to achieve sustainability can be identified from the existing literature. The first type is illustrated by Ye *et al.*, where biodegradable PLA was used with lignin and a lignin-based compatibilizer to achieve improved mechanical properties of the 3D-printed lignin materials.[96] In another work, a fully plant-based 3D-printed structure comprised of lignin and zein degraded readily in the presence of common bacteria found in the soil.[215] The degradation of the lignin–zein composite was faster than that of the biodegradable plastic (*i.e.* PLA). Another strategy is to establish the recyclability of the materials. For instance, lignin was developed into thermosets along with vanillin and soybean oil.[126] The 3D-printed lignin materials could self-heal, which extended the lifespan of the materials, thereby contributing to sustainability management. Indeed, this lifespan extension only delays the duration before the materials go into the waste pile, but at least the amount of waste generated is expected to be reduced. This is undoubtedly a feat to be acknowledged as it highlights a possible direction to work towards in the future (*i.e.* improves recyclability perhaps indefinitely).

6.3. Efficient use of lignin materials *via* additive manufacturing and their life-cycle assessment

After examining the different approaches that were undertaken to comply with the sustainability aim in lignin extraction/modification and biodegradability/recyclability of the 3D-printed lignin materials, it would be interesting to scrutinize the efficient use of lignin materials in additive manufacturing as compared to conventional subtractive manufacturing. Additive manufacturing involves layer-by-layer printing using 3D models,[88,216] whereas subtractive manufacturing relies on machining to remove materials to achieve the desired geometry.[216,217] The efficiency comparison can be achieved using the life cycle assessment (LCA). LCA is a comprehensive environmental tool that evaluates the impacts of a technology or a product from cradle to grave without having the adverse impacts shifted from one sector to another.[218] There are four segments in the LCA, which are (i) goal setting and scope definition, (ii) inventory analysis, (iii) impact assessment, and (iv) interpretation.

In this context, the goal is to evaluate the efficiency of using lignin materials *via* additive manufacturing compared to subtractive manufacturing by assessing its environmental burden, and the scope is from raw materials to the final product. The next step is to identify the inputs and outputs. Inputs required include but are not limited to lignin, chemicals, machines, energy, and resources. Outputs would be the emissions produced to the ecosystem. The inputs for additive/subtractive manufacturing may appear straightforward, but its representation in the LCA is much more complex. For instance, electricity is required for powering equipment such as a 3D printer or machinery; the 3D printer/machinery must be fabricated before additive/subtractive manufacturing, and the essential chemicals for the manufacturing will need to be extracted or synthesized before their use. LCA utilizes ReCiPe Endpoint and Midpoint methods to assess the impacts. The end-point indicators are damage-oriented, targeting three main areas, which are ecosystems, human health, and resources.[219] In contrast, mid-point indicators are more specific in terms of the damage, such as climate change, marine ecotoxicity, freshwater ecotoxicity, agricultural land occupation, urban land occupation, and water depletion. An unavoidable impact is the release of CO_2 from the burning of fossil fuels to power equipment, as fossil fuels are still the main energy sources. At present, the most common way to obtain lignin is through tapping into the pulp and paper industry, where lignin is generated as a by-product. Billions of cubic meters of water are estimated to have been consumed annually,[220] which fall under the water depletion indicator. Additionally, the polluted wastewater could cause marine ecotoxicity and freshwater ecotoxicity. While these are some common impacts shared by additive and subtracting manufacturing, there are still different impacts experienced by each type. For instance, the waste generated by additive manufacturing is highly likely to be much less than that generated by subtractive manufacturing, where the 3D structure is subjected to machining to remove unwanted parts. These wastes will likely compete for space, which falls under the agricultural and urban land occupation indicators. In contrast to subtractive manufacturing, layer-by-layer printing suggests that fewer reagent inputs are required, which could translate to less chemical synthesis/extraction and pollution. With the identification of the impacts, the last step is to interpret the information. Unfortunately, this LCA segment is not as comprehensive as it should be. There are no quantitative data, and there is no discussion on the region or the distance between the resources and the factory. These details, though important, are region-specific, and the impacts would differ accordingly. Instead, we would like to focus on the efficiency of using lignin materials for manufacturing.

The manufacturing process with more efficient use of lignin materials would be the one with fewer inputs required yet producing the same if not more outputs or the one with less waste generated. It is difficult to assess the former scenario as there are many ways and formulations to synthesize lignin-based materials. The only way to evaluate it is to specify the process as well as the inputs required and the outputs produced. As for the latter, the description of the manufacturing process suggests that additive manufacturing would produce less waste. In contrast, subtractive manufacturing removes materials to attain the desired geometry, which produces more material waste, even after considering the potential recycling of the subtracted materials in some cases. Hence, it is safe to assume that less waste would be generated in additive manufacturing, where lignin materials are used more efficiently.

7. Outlook and challenges

Although there have been many studies on lignin-related 3D printing, lignin is only adopted in limited volumes due to the deteriorated printability or mechanical properties with the addition of lignin. Enhanced printability and mechanical performance of lignin materials could be realized through the modification and pretreatment of lignin, improving the interfacial interaction between lignin and other polymers and leading to high adoption ratios of lignin in the 3D printing matrix. Meanwhile, from the sustainability point of view, waste minimization and avoiding toxic chemicals and complex processes should be prioritized when selecting and designing lignins for 3D printing. Here are a few points that need to be kept in mind for future work:

(1) Most existing work focuses on the use and modification of technical lignins; lignocellulose biomass containing 15–35% lignin for 3D printing is underutilized. The most challenging part of 3D/4D printing of lignin materials is to bring pure lignin or lignocellulose biomass to the dominant position regarding material ratios and their influence on the printing process and final properties. Meanwhile, considering the full utilization and valorization of lignocellulose biomass, 3D/4D printing of crude biomass should be prioritized in future work.

(2) Some lignocellulose biomass feedstocks are not long-term sustainable candidates if we consider the raised potential competition for the food supply or deforestation. The lignocellulose biomass sourced from agricultural wastes and food wastes, like coconut husk, coir fiber, sugarcane bagasse, pineapple leaf fibers, and durian peels, is the optimal feedstock of the material selection for 3D/4D printing. In the meantime, the upcycling and value-adding of these waste lignocellulose biomasses could be achieved.

(3) The variation in the properties of lignin/lignocellulose biomass from different sources or extraction methods further complicates 3D printing with lignin materials. The printing parameters should be carefully adjusted to achieve the optimal performance of 3D-printed lignin materials. For example, Sharma *et al.* proposed a novel nozzle design for FDM that can choose different extrusion points and dies of variable shapes, sizes, and cross-sections,[221] which can potentially accommodate different bio-composites with variable flow properties.

(4) Regarding the DIW, water remains the dominant medium for lignocellulose biomass treatment and preparation, in which harsh chemicals are often involved for optimal pretreatment. Water is the main medium for paste-like printable inks produced from lignin/lignocellulose. However, alternative green and sustainable solvents, like deep eutectic solvents (DES), should be explored for the pretreatment of lignin/lignocellulose biomass to make them suitable feedstocks and as media for paste-like inks for DIW 3D printing. Additionally, DES systems, particularly acrylic acid-based DES systems, facilitate the incorporation of lignin components into photopolymer systems, making them suitable for both SLA and DIW and enabling the formation of eutectogels.

(5) Lignin's intrinsic UV, visible, and near-infrared light absorption properties make it a promising candidate for sustainable photothermal conversion and enhanced control over SLA printing resolution. Additionally, the development of sustainable additives, such as modified lignin with intrinsic shape-memory or self-healing properties, presents significant potential for advancing 4D printing technologies in future research.

(6) More efforts should be made to explore more application scenarios for 3D-printed lignin materials. So far, significant work has only focused on optimizing printability and demonstrating 3D-printed objects. Some application demonstrations in previous work are not convincing, as 3D printing is unnecessary, and the demonstration could be realized using regular material preparation techniques, like mold-casting.

Author contributions

T. W., S. S., R. Y., T. S., U. A. W., P. L. C., and O. Y. prepared the draft. G. N. and D. K. reviewed and edited the manuscript. All authors have read and agreed to the published version of the manuscript.

Data availability

No primary research results, software or code have been included and no new data were generated or analysed as part of this review.

Conflicts of interest

The authors declare no conflict of interest.

Acknowledgements

This work is supported by the RIE2025 MTC Individual Research Grants (M22K2c0085), administered by the Agency of Science, Technology and Research (A*STAR), Singapore.

References

1 S. Jia, Z. Lv, J. Rao, B. Lu, G. Chen, J. Bian, M. Li and F. Peng, *ACS Nano*, 2023, **17**, 13627–13637.
2 X. Wang, Q. Xia, S. Jing, C. Li, Q. Chen, B. Chen, Z. Pang, B. Jiang, W. Gan, G. Chen, M. Cui, L. Hu and T. Li, *Small*, 2021, **17**, e2008011.
3 C. O. Tuck, E. Pérez, I. T. Horváth, R. A. Sheldon and M. Poliakoff, *Science*, 2012, **337**, 695–699.
4 Q. Xia, C. Chen, Y. Yao, J. Li, S. He, Y. Zhou, T. Li, X. Pan, Y. Yao and L. Hu, *Nat. Sustain.*, 2021, **4**, 627–635.
5 A. Shavandi, S. Hosseini, O. V. Okoro, L. Nie, F. Eghbali Babadi and F. Melchels, *Adv. Healthcare Mater.*, 2020, **9**, e2001472.
6 M. N. Collins, M. Nechifor, F. Tanasa, M. Zanoaga, A. McLoughlin, M. A. Strozyk, M. Culebras and C. A. Teaca, *Int. J. Biol. Macromol.*, 2019, **131**, 828–849.
7 B. Jiang, C. Chen, Z. Liang, S. He, Y. Kuang, J. Song, R. Mi, G. Chen, M. Jiao and L. Hu, *Adv. Funct. Mater.*, 2019, **30**, 1906307.
8 R. A. Sheldon, *J. Mol. Catal. A: Chem.*, 2016, **422**, 3–12.
9 A. Eraghi Kazzaz, Z. Hosseinpour Feizi and P. Fatehi, *Green Chem.*, 2019, **21**, 5714–5752.
10 E. A. Agustiany, M. Rasyidur Ridho, M. Rahmi, D. N. E. W. Madyaratri, F. Falah, M. A. R. Lubis, N. N. Solihat, F. A. Syamani, P. Karungamye, A. Sohail, D. S. Nawawi, A. H. Prianto, A. H. Iswanto, M. Ghozali, W. K. Restu, I. Juliana, P. Antov, L. Kristak, W. Fatriasari and A. Fudholi, *Polym. Compos.*, 2022, **43**, 4848–4865.
11 A. Y. Gebreyohannes, S. L. Aristizábal, L. Silva, E. A. Qasem, S. Chisca, L. Upadhyaya, D. Althobaiti, J. A. P. Coutinho and S. P. Nunes, *Green Chem.*, 2023, **25**, 4769–4780.
12 R. Liang, X. Yang, P. Y. M. Yew, S. Sugiarto, Q. Zhu, J. Zhao, X. J. Loh, L. Zheng and D. Kai, *J. Nanobiotechnol.*, 2022, **20**, 327.
13 N. A. Nguyen, Sietske H. Barnes, Christopher C. Bowland, Kelly M. Meek, Kenneth C. Littrell, Jong K. Keum and Amit K. Naskar, *Sci. Adv.*, 2018, **4**, eaat4967.
14 L. S. Ebers, A. Arya, C. C. Bowland, W. G. Glasser, S. C. Chmely, A. K. Naskar and M. P. Laborie, *Biopolymers*, 2021, **112**, e23431.
15 J. Dominguez-Robles, N. K. Martin, M. L. Fong, S. A. Stewart, N. J. Irwin, M. I. Rial-Hermida, R. F. Donnelly and E. Larraneta, *Pharmaceutics*, 2019, **11**, 165.
16 S. Wasti, E. Triggs, R. Farag, M. Auad, S. Adhikari, D. Bajwa, M. Li and A. J. Ragauskas, *Composites, Part B*, 2021, **205**, 108483.
17 A. A. Vaidya, C. Collet, M. Gaugler and G. Lloyd-Jones, *Mater. Today Commun.*, 2019, **19**, 286–296.
18 H. Ye, Y. He, H. Li, T. You and F. Xu, *Polymers*, 2023, **15**, 2806.
19 M. Tanase-Opedal, E. Espinosa, A. Rodriguez and G. Chinga-Carrasco, *Materials*, 2019, **12**, 3006.
20 J. T. Sutton, K. Rajan, D. P. Harper and S. C. Chmely, *ACS Appl. Mater. Interfaces*, 2018, **10**, 36456–36463.
21 B. Jiang, H. Jiao, X. Guo, G. Chen, J. Guo, W. Wu, Y. Jin, G. Cao and Z. Liang, *Adv. Sci.*, 2023, **10**, e2206055.
22 J. Yang, X. An, B. Lu, H. Cao, Z. Cheng, X. Tong, H. Liu and Y. Ni, *Int. J. Biol. Macromol.*, 2024, **267**, 131364.
23 C. Gauss, K. L. Pickering and L. P. Muthe, *Compos., Part C: Open Access*, 2021, **4**, 100113.
24 Y. Zhang, H. Wang, T. L. Eberhardt, Q. Gu and H. Pan, *Eur. Polym. J.*, 2021, **150**, 110389.
25 S. Vaz Jr and C. E. D. M. Salvador, *Sustainable Chem. Pharm.*, 2023, **36**, 101273.
26 X. Jiang, Z. Tian, X. Ji, H. Ma, G. Yang, M. He, L. Dai, T. Xu and C. Si, *Int. J. Biol. Macromol.*, 2022, **201**, 400–410.
27 G. J. Jiao, P. Peng, S. L. Sun, Z. C. Geng and D. She, *Int. J. Biol. Macromol.*, 2019, **127**, 544–554.

28 A. Eraghi Kazzaz and P. Fatehi, *J. Colloid Interface Sci.*, 2020, **561**, 231–243.
29 S. Hu, T. Zhang, B. Jiang, C. Huang, W. Wei, W. Wu and Y. Jin, *Bioresour. Technol.*, 2023, **384**, 129276.
30 W. Gao, J. P. W. Inwood and P. Fatehi, *J. Bioresour. Bioprod.*, 2019, **4**, 80–88.
31 A. Abbas, Z. Wang, Y. Zhang, P. Peng and D. She, *Int. J. Biol. Macromol.*, 2022, **222**, 1801–1817.
32 P. Figueiredo, K. Lintinen, J. T. Hirvonen, M. A. Kostiainen and H. A. Santos, *Prog. Mater. Sci.*, 2018, **93**, 233–269.
33 X. Zhang, S. Keck, Y. Qi, S. Baudis and Y. Zhao, *ACS Sustainable Chem. Eng.*, 2020, **8**, 10959–10970.
34 S. Laurichesse and L. Avérous, *Prog. Polym. Sci.*, 2014, **39**, 1266–1290.
35 Z. Dai, P.-G. Ren, W. He, X. Hou, F. Ren, Q. Zhang and Y.-L. Jin, *Renewable Energy*, 2020, **162**, 613–623.
36 L.-Y. Liu, Q. Hua and S. Renneckar, *Green Chem.*, 2019, **21**, 3682–3692.
37 A. L. Ruiz Deance, B. Siersema, L. E. A.-C. Yoe, F. R. Wurm and H. Gojzewski, *ACS Appl. Polym. Mater.*, 2023, **5**, 10021–10031.
38 C. Dong, X. Meng, S.-Y. Leu, L. Xu, Z. Wu, G. Cravotto and Z. Fang, *Ind. Crops Prod.*, 2022, **185**, 115130.
39 J. Cheng, C. Huang, Y. Zhan, S. Han, J. Wang, X. Meng, C. G. Yoo, G. Fang and A. J. Ragauskas, *Chem. Eng. J.*, 2022, **443**, 136395.
40 Y. Liu, X. Huang, K. Han, Y. Dai, X. Zhang and Y. Zhao, *ACS Sustainable Chem. Eng.*, 2019, **7**, 4004–4011.
41 Z. Zhang, Q. Liu, T. Gao, C. Qiao, J. Yao and C. Zhang, *J. Water Process. Eng*, 2022, **50**, 103334.
42 D. S. Bajwa, G. Pourhashem, A. H. Ullah and S. G. Bajwa, *Ind. Crops Prod.*, 2019, **139**, 111526.
43 B. Ahvazi, O. Wojciechowicz, T.-M. Ton-That and J. Hawari, *J. Agric. Food Chem.*, 2011, **59**, 10505–10516.
44 T. A. Lerma, E. M. Combatt and M. Palencia, *Eur. Polym. J.*, 2023, **198**, 112376.
45 M. Wu, M. Wu, M. Pan, F. Jiang, B. Hui and L. Zhou, *Int. J. Biol. Macromol.*, 2022, **207**, 522–530.
46 I. Zaborniak, A. Macior, P. Chmielarz, M. Caceres Najarro and J. Iruthayaraj, *Polymer*, 2021, **219**, 123537.
47 W. Huang, M. Wu, W. Liu, Z. Hua, Z. Wang and L. Zhou, *Appl. Surf. Sci.*, 2019, **475**, 302–311.
48 S. Gao, Z. Cheng, X. Zhou, Y. Liu, J. Wang, C. Wang, F. Chu, F. Xu and D. Zhang, *Chem. Eng. J.*, 2020, **394**, 124896.
49 Y. Ou, Y. Xing, Z. Yang, J. Huang, J. He, F. Jiang and Y. Zhang, *Int. J. Biol. Macromol.*, 2024, **256**, 128507.
50 Y. Xu, N. Li, G. Wang, C. Wang and F. Chu, *Polymers*, 2021, **13**, 968.
51 J. Perez-Arce, A. Centeno-Pedrazo, J. Labidi, J. R. Ochoa-Gomez and E. J. Garcia-Suarez, *Polymers*, 2021, **13**, 651.
52 R. V. Gadhave, P. S. Kasbe, P. A. Mahanwar and P. T. Gadekar, *Int. J. Adhes. Adhes.*, 2019, **95**, 102427.
53 Y.-Y. Wang, C. E. Wyman, C. M. Cai and A. J. Ragauskas, *ACS Appl. Polym. Mater.*, 2019, **1**, 1672–1679.
54 J. Sternberg and S. Pilla, *Green Chem.*, 2020, **22**, 6922–6935.
55 J. Sternberg and S. Pilla, *Nat. Sustain.*, 2023, **6**, 316–324.
56 S. Zhang, X. Meng, S. Bhagia, A. Ji, M. Dean Smith, Y.-Y. Wang, B. Liu, C. G. Yoo, D. P. Harper and A. J. Ragauskas, *Chem. Eng. J.*, 2024, **481**, 148449.
57 J. Yao, K. Odelius and M. Hakkarainen, *ACS Appl. Polym. Mater.*, 2021, **3**, 3538–3548.
58 G. Murillo-Morales, S. Sethupathy, M. Zhang, L. Xu, A. Ghaznavi, J. Xu, B. Yang, J. Sun and D. Zhu, *Int. J. Biol. Macromol.*, 2023, **236**, 123881.
59 H. Long, L. Hu, F. Yang, Q. Cai, Z. Zhong, S. Zhang, L. Guan, D. Xiao, W. Zheng, W. Zhou, Y. Wei, K. Frank and X. Dong, *Composites, Part B*, 2022, **239**, 109968.
60 S. Bhagia, R. R. Lowden, D. Erdman, M. Rodriguez, B. A. Haga, I. R. M. Solano, N. C. Gallego, Y. Pu, W. Muchero, V. Kunc and A. J. Ragauskas, *Appl. Mater. Today*, 2020, **21**, 100832.
61 S. Zhang, M. Li, N. Hao and A. J. Ragauskas, *ACS Omega*, 2019, **4**, 20197–20204.
62 X. Feng, Z. Yang, S. Chmely, Q. Wang, S. Wang and Y. Xie, *Carbohydr. Polym.*, 2017, **169**, 272–281.
63 D. Bocherer, R. Montazeri, Y. Li, S. Tisato, L. Hambitzer and D. Helmer, *Adv. Sci.*, 2024, **11**, 2406311.
64 J. Yao, M. Morsali, A. Moreno, M. H. Sipponen and M. Hakkarainen, *Eur. Polym. J.*, 2023, **194**, 112146.
65 I. Romero-Ocaña and S. I. Molina, *Addit. Manuf.*, 2022, **51**, 102586.
66 B. Jiang, Y. Yao, Z. Liang, J. Gao, G. Chen, Q. Xia, R. Mi, M. Jiao, X. Wang and L. Hu, *Small*, 2020, **16**, e1907212.
67 M. S. H. Thakur, Chen Shi, Logan T. Kearney, M. A. S. R. Saadi, Matthew D. Meyer, Amit K. Naskar, Pulickel M. Ajayan and M. M. Rahman, *Sci. Adv.*, 2024, **10**, eadk3250.
68 C. Liu, M.-C. Li, X. Liu, G. Zhou, C. Liu and C. Mei, *Addit. Manuf.*, 2023, **78**, 103841.
69 D. Kam, I. Levin, Y. Kutner, O. Lanciano, E. Sharon, O. Shoseyov and S. Magdassi, *Polymers*, 2022, **14**, 733.
70 R. Ajdary, N. Kretzschmar, H. Baniasadi, J. Trifol, J. V. Seppälä, J. Partanen and O. J. Rojas, *ACS Sustainable Chem. Eng.*, 2021, **9**, 2727–2735.
71 Z. Ren, K. Ding, X. Zhou, T. Ji, H. Sun, X. Chi and M. Xu, *Int. J. Biol. Macromol.*, 2023, **253**, 126562.
72 W. J. Grigsby, S. M. Scott, M. I. Plowman-Holmes, P. G. Middlewood and K. Recabar, *Acta Biomater.*, 2020, **104**, 95–103.
73 O. A. Mohamed, S. H. Masood and J. L. Bhowmik, *Adv. Manuf.*, 2015, **3**, 42–53.
74 O. S. Carneiro, A. F. Silva and R. Gomes, *Mater. Des.*, 2015, **83**, 768–776.
75 M. E. Mackay, Z. R. Swain, C. R. Banbury, D. D. Phan and D. A. Edwards, *J. Rheol.*, 2017, **61**, 229–236.
76 N. A. Nguyen, S. H. Barnes, C. C. Bowland, K. M. Meek, K. C. Littrell, J. K. Keum and A. K. Naskar, *Sci. Adv.*, 2018, **4**, eaat4967.
77 J. O. Obielodan, M. Delwiche, D. Clark, C. Downing, D. Huntoon and T. Wu, *J. Eng. Mater. Technol.*, 2021, **144**, 021009.

78 S. Domenek, A. Louaifi, A. Guinault and S. Baumberger, *J. Polym. Environ.*, 2013, **21**, 692–701.

79 O. Gordobil, I. Egüés, R. Llano-Ponte and J. Labidi, *Polym. Degrad. Stab.*, 2014, **108**, 330–338.

80 M. A. S. Anwer, H. E. Naguib, A. Celzard and V. Fierro, *Composites, Part B*, 2015, **82**, 92–99.

81 C.-W. Park, W.-J. Youe, S.-J. Kim, S.-Y. Han, J.-S. Park, E.-A. Lee, G.-J. Kwon, Y.-S. Kim, N.-H. Kim and S.-H. Lee, *Polymers*, 2019, **11**, 2089.

82 R. Kumar Singla, S. N. Maiti and A. K. Ghosh, *Polym.-Plast. Technol. Eng.*, 2016, **55**, 475–485.

83 V. Mimini, E. Sykacek, S. N. A. Syed Hashim, J. Holzweber, H. Hettegger, K. Fackler, A. Potthast, N. Mundigler and T. Rosenau, *J. Wood Chem. Technol.*, 2019, **39**, 14–30.

84 E. Gkartzou, E. P. Koumoulos and C. A. Charitidis, *Manuf. Rev.*, 2017, **4**, 1.

85 Z. Ren, X. Zhou, K. Ding, T. Ji, H. Sun, X. Chi, Y. Wei, M. Xu, L. Cai and C. Xia, *Int. J. Biol. Macromol.*, 2023, **253**, 127264.

86 H. Anuar, N. A. A. Rahman, M. R. Manshor, Y. A. Alli, O. A. Alimi, F. Alif and J. Suhr, *Mater. Today Commun.*, 2023, **35**, 106093.

87 N. A. Nguyen, C. C. Bowland and A. K. Naskar, *Data Brief*, 2018, **19**, 936–950.

88 N. A. Nguyen, C. C. Bowland and A. K. Naskar, *Appl. Mater. Today*, 2018, **12**, 138–152.

89 K. Akato, C. D. Tran, J. Chen and A. K. Naskar, *ACS Sustainable Chem. Eng.*, 2015, **3**, 3070–3076.

90 D. Mohan, A. N. Bakir, M. S. Sajab, S. B. Bakarudin, N. N. Mansor, R. Roslan and H. Kaco, *Polym. Compos.*, 2021, **42**, 2408–2421.

91 X. Zhou, Z. Ren, H. Sun, H. Bi, T. Gu and M. Xu, *Int. J. Biol. Macromol.*, 2022, **221**, 1209–1217.

92 Q. Yu, A. Bahi and F. Ko, *Macromol. Mater. Eng.*, 2015, **300**, 1023–1032.

93 S. H. Hong, J. H. Park, O. Y. Kim and S. H. Hwang, *Polymers*, 2021, **13**, 667.

94 S. Zhang, X. Meng, S. Bhagia, A. Ji, M. Dean Smith, Y.-Y. Wang, B. Liu, C. Geun Yoo, D. P. Harper and A. J. Ragauskas, *Chem. Eng. J.*, 2024, **481**, 148449.

95 L. Liu, M. Lin, Z. Xu and M. Lin, *BioResources*, 2019, **14**, 8484–8498.

96 H. Ye, Y. He, H. Li, T. You and F. Xu, *Ind. Crops Prod.*, 2023, **205**, 117454.

97 G. Murillo-Morales, S. Sethupathy, M. Zhang, L. Xu, A. Ghaznavi, J. Xu, B. Yang, J. Sun and D. Zhu, *Int. J. Biol. Macromol.*, 2023, **236**, 123881.

98 Y. Sun, L. Yang, X. Lu and C. He, *J. Mater. Chem. A*, 2015, **3**, 3699–3709.

99 R. Ding, Z. Duan, Y. Sun, Q. Yuan, T. T. Tien, M. G. Zúniga, E. Oh, J.-D. Nam and J. Suhr, *Ind. Crops Prod.*, 2023, **194**, 116286.

100 L. Hu, H. Long, F. Yang, Q. Cai, Y. Wu, Z. Li, J. Xiao, D. Xiao, S. Zhang, L. Guan, W. Zheng, W. Zhou and X. Dong, *Polym. Compos.*, 2022, **43**, 6817–6828.

101 M. Kariz, M. Sernek, M. Obućina and M. K. Kuzman, *Mater. Today Commun.*, 2018, **14**, 135–140.

102 A. Le Duigou, M. Castro, R. Bevan and N. Martin, *Mater. Des.*, 2016, **96**, 106–114.

103 S. Guessasma, S. Belhabib and H. Nouri, *Polymers*, 2019, **11**, 1220.

104 Y. Dong, J. Milentis and A. Pramanik, *Adv. Manuf.*, 2018, **6**, 71–82.

105 Z. Liu, Q. Lei and S. Xing, *J. Mater. Res. Technol.*, 2019, **8**, 3741–3751.

106 P. Li, L. Pan, D. Liu, Y. Tao and S. Q. Shi, *Materials*, 2019, **12**, 2896.

107 N. Ayrilmis, *Polym. Test.*, 2018, **71**, 163–166.

108 N. Ayrilmis, M. Kariz, J. H. Kwon and M. Kitek Kuzman, *Int. J. Adv. Des. Manuf. Technol.*, 2019, **102**, 2195–2200.

109 K. Vigneshwaran and N. Venkateshwaran, *Int. J. Polym. Anal. Charact.*, 2019, **24**, 584–596.

110 J. A. Taborda-Ríos, O. López-Botello, P. Zambrano-Robledo, L. A. Reyes-Osorio and C. Garza, *J. Reinf. Plast. Compos.*, 2020, **39**, 932–944.

111 K. E. Mazur, A. Borucka, P. Kaczor, S. Gądek, R. Bogucki, D. Mirzewiński and S. Kuciel, *J. Polym. Environ.*, 2022, **30**, 2341–2354.

112 M. Muller, P. Jirku, V. Sleger, R. K. Mishra, M. Hromasova and J. Novotny, *Polymers*, 2022, **14**, 4930.

113 N. Gama, S. Magina, A. Ferreira and A. Barros-Timmons, *Polym. J.*, 2021, **53**, 1459–1467.

114 X. Song, W. He, S. Yang, G. Huang and T. Yang, *Appl. Sci.*, 2019, **9**, 4892.

115 H. Liu, H. He, X. Peng, B. Huang and J. Li, *Polym. Adv. Technol.*, 2019, **30**, 910–922.

116 W. Yu, L. Dong, W. Lei, Y. Zhou, Y. Pu and X. Zhang, *Molecules*, 2021, **26**, 3234.

117 Z. Ni, J. Shi, M. Li, W. Lei and W. Yu, *Polymers*, 2023, **15**, 2382.

118 J. T. Sutton, K. Rajan, D. P. Harper and S. C. Chmely, *Polymers*, 2021, **13**, 3473.

119 Y. Bao, *Macromol. Rapid Commun.*, 2022, **43**, e2200202.

120 G. Arias-Ferreiro, A. Lasagabaster-Latorre, A. Ares-Pernas, P. Ligero, S. M. Garcia-Garabal, M. S. Dopico-Garcia and M. J. Abad, *Polymers*, 2022, **14**, 4164.

121 I. Romero-Ocaña, N. F. Delgado and S. I. Molina, *Ind. Crops Prod.*, 2022, **189**, 115832.

122 F. Ibrahim, D. Mohan, M. S. Sajab, S. B. Bakarudin and H. Kaco, *Polymers*, 2019, **11**, 1544.

123 S. Keck, O. Liske, K. Seidler, B. Steyrer, C. Gorsche, S. Knaus and S. Baudis, *Biomacromolecules*, 2023, **24**, 1751–1762.

124 X. Zhang, S. Keck, Y. Qi, S. Baudis and Y. Zhao, *ACS Sustainable Chem. Eng.*, 2020, **8**, 10959–10970.

125 L. Wang, Q. Wang, A. Slita, O. Backman, Z. Gounani, E. Rosqvist, J. Peltonen, S. Willför, C. Xu, J. M. Rosenholm and X. Wang, *Green Chem.*, 2022, **24**, 2129–2145.

126 R. M. Johnson, K. P. Cortés-Guzmán, S. D. Perera, A. R. Parikh, V. Ganesh, W. E. Voit and R. A. Smaldone, *J. Polym. Sci.*, 2023, **62**, 2585–2596.

127 X. Feng, Z. Yang, S. Chmely, Q. Wang, S. Wang and Y. Xie, *Carbohydr. Polym.*, 2017, **169**, 272–281.

128 X. Feng, Z. Yang, S. Wang and Z. Wu, *Polym. Eng. Sci.*, 2022, **62**, 2968–2976.
129 S. Zhang, S. Bhagia, M. Li, X. Meng and A. J. Ragauskas, *Mater. Des.*, 2021, **206**, 109773.
130 J. Yao and M. Hakkarainen, *Compos. Commun.*, 2023, **38**, 101506.
131 X. Lu and X. Gu, *Int. J. Biol. Macromol.*, 2023, **229**, 778–790.
132 A. C. H. Tsang, J. Zhang, K. N. Hui, K. S. Hui and H. Huang, *Adv. Mater. Technol.*, 2022, **7**, 2101358.
133 A. Moreno and M. H. Sipponen, *Mater. Horiz.*, 2020, **7**, 2237–2257.
134 J. Roman, W. Neri, V. Fierro, A. Celzard, A. Bentaleb, I. Ly, J. Zhong, A. Derré and P. Poulin, *Nano Today*, 2020, **33**, 100881.
135 B. D. Mattos, N. Jäntti, S. Khakalo, Y. Zhu, A. Miettinen, J. Parkkonen, A. Khakalo, O. J. Rojas and M. Ago, *Adv. Funct. Mater.*, 2023, **33**, 2304867.
136 F. R. Gleuwitz, G. Sivasankarapillai, G. Siqueira, C. Friedrich and M. G. Laborie, *ACS Appl. Bio Mater.*, 2020, **3**, 6049–6058.
137 H. Baniasadi, R. Ajdary, J. Trifol, O. J. Rojas and J. Seppala, *Carbohydr. Polym.*, 2021, **266**, 118114.
138 B. Jiang, H. Huang, W. Gong, X. Gu, T. Liu, J. Zhang, W. Qin, H. Chen, Y. Jin, Z. Liang and L. Jiang, *Adv. Funct. Mater.*, 2021, **31**, 2105045.
139 X. Zhang, M. Morits, C. Jonkergouw, A. Ora, J. J. Valle-Delgado, M. Farooq, R. Ajdary, S. Huan, M. Linder, O. Rojas, M. H. Sipponen and M. Osterberg, *Biomacromolecules*, 2020, **21**, 1875–1885.
140 S. Nida, J. A. Moses and C. Anandharamakrishnan, *Biomass Convers. Biorefin.*, 2021, 1–11, DOI: 10.1007/s13399-021-01982-0.
141 E. Gokce Bahcegul, E. Bahcegul and N. Ozkan, *Ind. Crops Prod.*, 2022, **186**, 115234.
142 S. Wang, L. Zhang, R. Ma, J. Yu, X. Zhang, C. Shi, L. Ma, T. Li, Y. Huang, Y. Hu, Y. Fan and Z. Wang, *Chem. Eng. J.*, 2023, **454**, 140022.
143 C. W. Lai and S. S. Yu, *ACS Appl. Mater. Interfaces*, 2020, **12**, 34235–34244.
144 H. Zhang, Y. Guo, K. Jiang, D. L. Bourell, D. Zhao, Y. Yu, P. Wang and Z. Li, A review of selective laser sintering of wood-plastic composites, *2016 International Solid Freeform Fabrication Symposium*, 2016.
145 Y. Guo, W. Zeng and K. Jiang, *Dig. J. Nanomater. Bios.*, 2011, **6**, 1435–1444.
146 A. Alzagameem, S. E. Klein, M. Bergs, X. T. Do, I. Korte, S. Dohlen, C. Hüwe, J. Kreyenschmidt, B. Kamm, M. Larkins and M. Schulze, *Polymers*, 2019, **11**, 670.
147 M. Behl and A. Lendlein, *Mater. Today*, 2007, **10**, 20–28.
148 X. Jin, X. Liu, X. Li, L. Du, L. Su, Y. Ma and S. Ren, *Int. J. Biol. Macromol.*, 2022, **219**, 44–52.
149 X. Jin, L. Du, X. Liu, J. Zhan, Y. Ma, S. Li and S. Ren, *ACS Appl. Polym. Mater.*, 2023, **5**, 7831–7840.
150 L.-Y. Liu, M. A. Karaaslan, Q. Hua, M. Cho, S. Chen and S. Renneckar, *Ind. Eng. Chem. Res.*, 2021, **60**, 11882–11892.
151 S. Wang and M. W. Urban, *Nat. Rev. Mater.*, 2020, **5**, 562–583.
152 N. Sun, Z. Wang, X. Ma, K. Zhang, Z. Wang, Z. Guo, Y. Chen, L. Sun, W. Lu, Y. Liu and M. Di, *Ind. Crops Prod.*, 2021, **174**, 114178.
153 X. Han, Y. Su, G. Che, Q. Wei, H. Zheng, J. Zhou and Y. Li, *ACS Appl. Mater. Interfaces*, 2022, **14**, 50199–50214.
154 B. Xue, R. Tang, D. Xue, Y. Guan, Y. Sun, W. Zhao, J. Tan and X. Li, *Ind. Crops Prod.*, 2021, **168**, 113583.
155 J. Zheng, Z. M. Png, S. H. Ng, G. X. Tham, E. Ye, S. S. Goh, X. J. Loh and Z. Li, *Mater. Today*, 2021, **51**, 586–625.
156 Z. Lyu, J. Wang and Y. Chen, *Int. J. Extreme Manuf.*, 2023, **5**, 032011.
157 S. Yan, F. Zhang, L. Luo, L. Wang, Y. Liu and J. Leng, *Research*, 2023, **6**, 0234.
158 A. Le Duigou, D. Correa, M. Ueda, R. Matsuzaki and M. Castro, *Mater. Des.*, 2020, **194**, 108911.
159 Z. Ren, X. Zhou, K. Ding, T. Ji, H. Sun, X. Chi, Y. Wei and M. Xu, *Ind. Crops Prod.*, 2024, **208**, 117809.
160 F. Suo, X. Bai, Y. Liu, M. Xu, T. Gu, L. Cao, X. Lv, X. Zhang and Y. Yao, *Int. J. Biol. Macromol.*, 2024, 132943, DOI: 10.1016/j.ijbiomac.2024.132943.
161 F. Wang, M. Jiang, Y. Pan, Y. Lu, W. Xu and Y. Zhou, *Polym. Test.*, 2023, **119**, 107934.
162 M. H. Tran, D.-P. Phan and E. Y. Lee, *Green Chem.*, 2021, **23**, 4633–4646.
163 W. Xu, X. Wang, N. Sandler, S. Willfor and C. Xu, *ACS Sustainable Chem. Eng.*, 2018, **6**, 5663–5680.
164 F. H. Graichen, W. J. Grigsby, S. J. Hill, L. G. Raymond, M. Sanglard, D. A. Smith, G. J. Thorlby, K. M. Torr and J. M. Warnes, *Ind. Crops Prod.*, 2017, **106**, 74–85.
165 D. Veeman, M. S. Sai, P. Sureshkumar, T. Jagadeesha, L. Natrayan, M. Ravichandran and W. D. Mammo, *Int. J. Polym. Sci.*, 2021, 1–20.
166 J. Yang, X. An, L. Liu, S. Tang, H. Cao, Q. Xu and H. Liu, *Carbohydr. Polym.*, 2020, **250**, 116881.
167 D. Kai, W. Ren, L. Tian, P. L. Chee, Y. Liu, S. Ramakrishna and X. J. Loh, *ACS Sustainable Chem. Eng.*, 2016, **4**, 5268–5276.
168 N. C. Hunt and L. M. Grover, *Biotechnol. Lett.*, 2010, **32**, 733–742.
169 H. N. Chia and B. M. Wu, *J. Biol. Eng.*, 2015, **9**, 1–14.
170 K. Smetana Jr, *Biomaterials*, 1993, **14**, 1046–1050.
171 N. Yanamala, E. R. Kisin, A. L. Menas, M. T. Farcas, T. O. Khaliullin, U. B. Vogel, G. V. Shurin, D. Schwegler-Berry, P. M. Fournier and A. Star, *Biomacromolecules*, 2016, **17**, 3464–3473.
172 S. Quraishi, M. Martins, A. A. Barros, P. Gurikov, S. Raman, I. Smirnova, A. R. C. Duarte and R. L. Reis, *J. Supercrit. Fluids*, 2015, **105**, 1–8.
173 J. Domínguez-Robles, N. K. Martin, M. L. Fong, S. A. Stewart, N. J. Irwin, M. I. Rial-Hermida, R. F. Donnelly and E. Larrañeta, *Pharmaceutics*, 2019, **11**, 165.
174 M. Giese, L. K. Blusch, M. K. Khan and M. J. MacLachlan, *Angew. Chem., Int. Ed.*, 2015, **54**, 2888–2910.
175 F. Oveissi, S. Naficy, T. Y. L. Le, D. F. Fletcher and F. Dehghani, *ACS Appl. Bio Mater.*, 2018, **1**, 2073–2081.

176 X. Zhang, M. Morits, C. Jonkergouw, A. Ora, J. J. Valle-Delgado, M. Farooq, R. Ajdary, S. Huan, M. Linder and O. Rojas, *Biomacromolecules*, 2020, **21**, 1875–1885.

177 J. Domínguez-Robles, E. Cuartas-Gómez, S. Dynes, E. Utomo, Q. K. Anjani, U. Detamornrat, R. F. Donnelly, N. Moreno-Castellanos and E. Larrañeta, *Sustainable Mater. Technol.*, 2023, **35**, e00581.

178 X. Wu, J. Jiang, C. Wang, J. Liu, Y. Pu, A. Ragauskas, S. Li and B. Yang, *Biofuels, Bioprod. Biorefin.*, 2020, **14**, 650–672.

179 J. Zhu, C. Yan, X. Zhang, C. Yang, M. Jiang and X. Zhang, *Prog. Energy Combust. Sci.*, 2020, **76**, 100788.

180 F. Temerov, A. Belyaev, B. Ankudze and T. T. Pakkanen, *J. Lumin.*, 2019, **206**, 403–411.

181 Z. Ding, F. Li, J. Wen, X. Wang and R. Sun, *Green Chem.*, 2018, **20**, 1383–1390.

182 J. Roman, W. Neri, V. Fierro, A. Celzard, A. Bentaleb, I. Ly, J. Zhong, A. Derré and P. Poulin, *Nano Today*, 2020, **33**, 100881.

183 Y. Shao, C. Guizani, P. Grosseau, D. Chaussy and D. Beneventi, *Composites, Part B*, 2018, **149**, 206–215.

184 S. Wang, Y. Yu, S. Luo, X. Cheng, G. Feng, Y. Zhang, Z. Wu, G. Compagnini, J. Pooran and A. Hu, *Appl. Phys. Lett.*, 2019, **115**, 083904.

185 F. Mahmood, H. Zhang, J. Lin and C. Wan, *ACS Omega*, 2020, **5**, 14611–14618.

186 R. Ye, Y. Chyan, J. Zhang, Y. Li, X. Han, C. Kittrell and J. M. Tour, *Adv. Mater.*, 2017, **29**, 1702211.

187 W. Zhang, Y. Lei, F. Ming, Q. Jiang, P. M. Costa and H. N. Alshareef, *Adv. Energy Mater.*, 2018, **8**, 1801840.

188 P. Cheng, S. Chen, X. Li, Y. Xu, F. Xu and A. J. Ragauskas, *Energy Convers. Manage.*, 2022, **255**, 115321.

189 J. Ye, Y. Cheng, L. Sun, M. Ding, C. Wu, D. Yuan, X. Zhao, C. Xiang and C. Jia, *J. Membr. Sci.*, 2019, **572**, 110–118.

190 B. Jiang, H. Huang, W. Gong, X. Gu, T. Liu, J. Zhang, W. Qin, H. Chen, Y. Jin and Z. Liang, *Adv. Funct. Mater.*, 2021, **31**, 2105045.

191 B. Jiang, Y. Yao, Z. Liang, J. Gao, G. Chen, Q. Xia, R. Mi, M. Jiao, X. Wang and L. Hu, *Small*, 2020, **16**, 1907212.

192 G. Arias-Ferreiro, A. Ares-Pernas, A. Lasagabáster-Latorre, M. S. Dopico-García, P. Ligero, N. Pereira, P. Costa, S. Lanceros-Mendez and M. J. Abad, *Adv. Mater. Technol.*, 2022, **7**, 2101503.

193 Z. Yu, Y. Wang, J. Zheng, Y. Xiang, P. Zhao, J. Cui, H. Zhou and D. Li, *Nano Energy*, 2020, **68**, 104382.

194 L. L. Kosbar, J. D. Gelorme, R. M. Japp and W. T. Fotorny, *J. Ind. Ecol.*, 2008, **4**, 93–105.

195 A. Kylili, M. Koutinas, P.-Z. Georgali and P. A. Fokaides, *Int. J. Renewable Sustainable Energy*, 2023, **42**, 1008–1027.

196 A. Ovejero-Pérez, V. Rigual, J. C. Domínguez, M. V. Alonso, M. Oliet and F. Rodriguez, *Int. J. Biol. Macromol.*, 2020, **157**, 461–469.

197 A. M. Asim, M. Uroos and N. Muhammad, *RSC Adv.*, 2020, **10**, 44003–44014.

198 T. J. Szalaty, L. Klapiszewski and T. Jesionowski, *J. Mol. Liq.*, 2020, **301**, 112417.

199 R. Lou and X. Zhang, *Bioresour. Technol.*, 2022, **344**, 126174.

200 Z. Chen, A. Ragauskas and C. Wan, *Ind. Crops Prod.*, 2020, **147**, 112241.

201 Á. Lobato-Rodríguez, B. Gullón, A. Romaní, P. Ferreira-Santos, G. Garrote and P. G. Del-Río, *Bioresour. Technol.*, 2023, **388**, 129744.

202 X. Liu, T. Li, S. Wu, H. Ma and Y. Yin, *Bioresour. Technol.*, 2020, **310**, 123460.

203 D. da Silva Vilar, M. Bilal, R. N. Bharagava, A. Kumar, A. Kumar Nadda, G. R. Salazar-Banda, K. I. B. Eguiluz and L. F. Romanholo Ferreira, *J. Chem. Technol. Biotechnol.*, 2022, **97**, 327–342.

204 L.-Y. Liu, X. Wan, S. Chen, P. Boonthamrongkit, M. Sipponen and S. Renneckar, *ChemSusChem*, 2023, **16**, e202300276.

205 L.-Y. Liu, S. Chen, L. Ji, S.-K. Jang and S. Renneckar, *Green Chem.*, 2021, **23**, 4567–4579.

206 D. Ahuja, A. Kaushik and M. Singh, *Int. J. Biol. Macromol.*, 2018, **107**, 1294–1301.

207 S. Angelini, D. Ingles, M. Gelosia, P. Cerruti, E. Pompili, G. Scarinzi, G. Cavalaglio, F. Cotana and M. Malinconico, *J. Cleaner Prod.*, 2017, **151**, 152–162.

208 C.-Y. Ma, L.-H. Xu, Q. Sun, X.-J. Shen, J.-L. Wen and T.-Q. Yuan, *Chem. Eng. J.*, 2022, **450**, 138315.

209 D. S. Zijlstra, C. W. Lahive, C. A. Analbers, M. B. Figueirêdo, Z. Wang, C. S. Lancefield and P. J. Deuss, *ACS Sustainable Chem. Eng.*, 2020, **8**, 5119–5131.

210 J.-Y. Yang, T.-S. Guo, Y.-H. Xu, M.-F. Li and J. Bian, *Ind. Crops Prod.*, 2023, **194**, 116269.

211 M. Mohan, K. Huang, V. R. Pidatala, B. A. Simmons, S. Singh, K. L. Sale and J. M. Gladden, *Green Chem.*, 2022, **24**, 1165–1176.

212 S. Kwon, M. C. Zambrano, J. J. Pawlak and R. A. Venditti, *Cellulose*, 2021, **28**, 2863–2877.

213 W. Li, S. Ma, L. Luo, Z. Li, A. He, C. Wang, L. Lin and X. Zeng, *Int. J. Biol. Macromol.*, 2024, **276**, 133751.

214 X. Zhou, Z. Ren, H. Sun, H. Bi, T. Gu and M. Xu, *Int. J. Biol. Macromol.*, 2022, **221**, 1209–1217.

215 J. G. Lee, Y. Guo, J. A. Belgodere, A. Al Harraq, A. A. Hymel, A. J. Pete, K. T. Valsaraj, M. G. Benton, M. G. Miller, J. P. Jung and B. Bharti, *ACS Sustainable Chem. Eng.*, 2021, **9**, 1781–1789.

216 H. Jayawardane, I. J. Davies, J. R. Gamage, M. John and W. K. Biswas, *Sustainable Manuf. Serv. Econ.*, 2023, **2**, 100015.

217 S. T. Newman, Z. Zhu, V. Dhokia and A. Shokrani, *CIRP Ann.*, 2015, **64**, 467–470.

218 A. Tukker, *Environ. Impact Assess. Rev.*, 2000, **20**, 435–456.

219 A. Rashedi and T. Khanam, *Environ. Sci. Pollut. Res.*, 2020, **27**, 29075–29090.

220 R. Toczyłowska-Mamińska, *Renewable Sustainable Energy Rev.*, 2017, **78**, 764–772.

221 V. Sharma, H. Roozbahani, M. Alizadeh and H. Handroos, *IEEE Access*, 2021, **9**, 57107–57119.